We are IntechOpen, the world's leading publisher of Open Access books
Built by scientists, for scientists

4,800
Open access books available

122,000
International authors and editors

135M
Downloads

154
Countries delivered to

Our authors are among the

TOP 1%
most cited scientists

12.2%
Contributors from top 500 universities

WEB OF SCIENCE™

Selection of our books indexed in the Book Citation Index
in Web of Science™ Core Collection (BKCI)

Interested in publishing with us?
Contact book.department@intechopen.com

Numbers displayed above are based on latest data collected.
For more information visit www.intechopen.com

Petrography, Geochemistry and Petrogenesis of Late-Stage Granites: An Example from the Glen Eden Area, New South Wales, Australia

A. K. Somarin

Department of Geology, Brandon University, Brandon, Manitoba, Canada

1. Introduction

The Glen Eden area is located within the New England Orogen (also known as New England Fold Belt). This orogen is one of the major structural elements within the extensive Tasman Orogenic Province which comprises the eastern part of the Australian continent (Hensel, 1982). The present length of this orogen is about 1500 km from Townsville to Newcastle. It is separated from the Thomson and Lachlan fold belts to the west by the Permian and Triassic strata of the Bowen-Gunnedah-Sydney Basin. The Mesozoic Clarence-Moreton and Great Artesian basins separate the northern and southern parts of this orogen.

The New England Orogen was the site of the extensive episodic calc-alkaline magmatism related to west-dipping subduction from middle Paleozoic to Early Cretaceous time. The oldest rocks might have formed at least partly in a volcanic island arc, but from the Late Devonian, the orogen developed as a convergent Pacific-type continental margin. During Late Devonian-Carboniferous time, parallel belts representing continental margin, volcanic arc, forearc basin and subduction complex assemblages can be recognized (Murray, 1988).

More than one hundred plutons were emplaced from the Late Carboniferous to the Triassic in the southern NEO. These intrusions have been attributed to two major periods of plutonism, the first during Late Carboniferous time and the second during the Late Permian and Triassic. The resulting plutons comprise the New England Batholith. Although volcanogenic massive sulfides and volcanic-hosted epithermal gold-silver ore deposits occur in older rock sequences (Murray, 1988), almost all of the other ore deposits of this region, including the Glen Eden Mo-W-Sn deposit, have a genetic or paragenetic relationship with plutons of the New England Batholith which is one of the largest Paleozoic-Mesozoic batholiths in eastern Australia. It underlies an area of almost 20000 km² and is composed of more than one hundred N-S-trending plutons which include all of the granitoids in the southern part of the NEO. These granitoids intruded into the tectono-stratigraphic terranes (Flood and Aitchison, 1993a, b) and deformed trench-complex metasedimentary rocks (Shaw and Flood, 1981). The composition of this batholith is 80% monzogranite, 18% granodiorite, 1% diorite and tonalite, 1% quartz-bearing monzonite and <0.2% gabbro (see Shaw and Flood, 1981).

On the basis of petrography, geochemistry and isotopic characteristics, Shaw and Flood (1981) subdivided the granitoids of the New England Batholith into five intrusive suites and

a group of leucoadamellites. They pointed out that the differences between these six groups reflect differences in their source rock types.

The Glen Eden Granite (GEG) occurs as dykes at depths of more than 80 m and is not exposed at the surface (Fig. 1). Mineralogical studies and field evidence indicate that the observed dykes have intruded after initiation of the hydrothermal activity. Based on petrographic studies, three types of GEG can be recognized: microgranite porphyry, micrographic granite, and aplite. Petrographic features of these granites are discussed below.
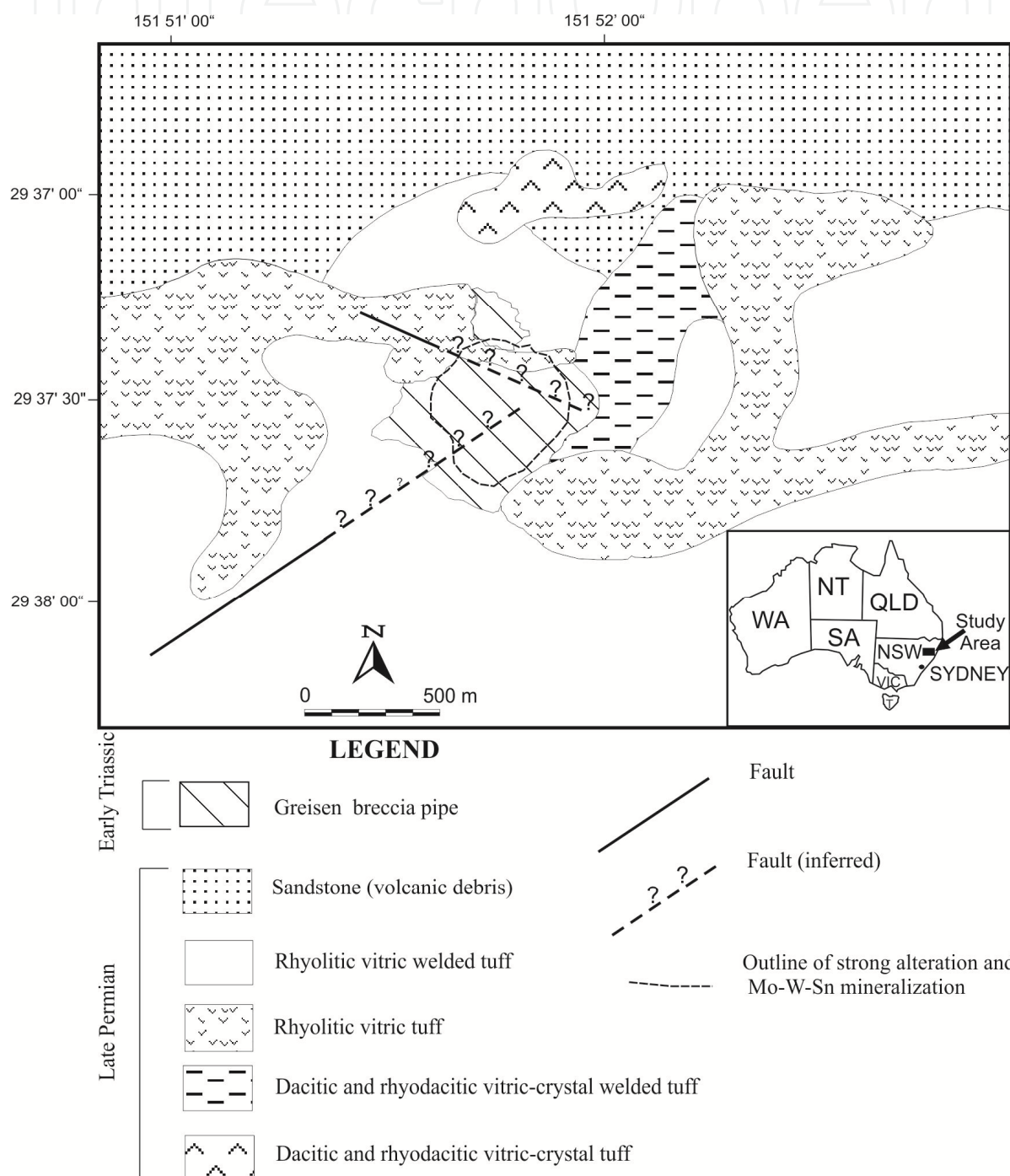

Fig. 1. Geological map of the Glen Eden area (after Somarin and Ashley, 2004).

2. Petrography of the Glen Eden granite

2.1 Microgranite porphyry

Microgranite porphyry of GEG is composed of quartz, K-feldspar and plagioclase as major minerals and biotite, zircon, xenotime, monazite and fluorite as accessory phases. Its texture is granular with quartz, K-feldspar, plagioclase and biotite as phenocrysts up to 8 mm in size. The groundmass is composed of quartz, K-feldspar and plagioclase, typically 50 to 300 µm, average 200 µm, in size. Most of the phenocrysts have irregular margins due to resorption and replacement by the groundmass. The cracks and embayments in these phenocrysts have been filled by the groundmass.

Quartz occurs as anhedral to euhedral grains, commonly rounded in shape and forming mosaics within feldspathic matrix. Some quartz grains form well-developed euhedral crystals, possibly due to secondary overgrowth. The presence of quartz as inclusions within biotite, plagioclase and fluorite and replacement of quartz phenocrysts by groundmass suggest that quartz crystallized relatively early.

K-feldspar is mostly orthoclase ($Or_{86}Ab_{14}$ to $Or_{98}Ab_2$) and mainly occurs as cloudy or perthitic anhedral crystals up to 5 mm in size. Rare microcline occurs as anhedral to subhedral grains 200-300 µm across. Perthitic hydrothermal K-feldspar in veins is common.

Plagioclase is mostly albitic ($Ab_{85}Or_{13}An_2$ to $Ab_{99}Or_1$) and occurs as subhedral to euhedral crystals and varies in size from 80-200 µm in groundmass up to 1.5-2.2 mm as phenocrysts. There is no zoning. In altered samples, the presence of K-feldspar as replacement rims around plagioclase implies sub-solidus alteration of plagioclase.

Biotite is dark brown to brown in color, strongly pleochroic and is mainly siderophyllite in composition. This mineral occurs as euhedral flakes, 50 µm up to a few millimeters in size. Commonly, biotite flakes have inclusions of magmatic quartz, zircon, xenotime, monazite and, in some samples, fluorite, rutile and secondary goethite accompany these flakes. These features are similar to those of Climax-type intrusives (e.g. White et al., 1981). Biotite is inferred to have been the most unstable mineral during hydrothermal alteration and commonly is replaced by sericite and goethite. Mostly, due to this replacement, only relics of biotite can be seen and its color changes from brown to cream. Based on textural criteria, the position of biotite in the crystallization sequence cannot be determined unequivocally. However, the interstitial nature of biotite in GEG and occurrence of other minerals as inclusions within it are indicative of its late crystallization which is consistent with a high activity of F during crystallization (see below; Munoz and Ludington, 1974; Tischendorf, 1977; Collins et al., 1982).

Locally, muscovite occurs as flakes in samples adjacent to hydrothermal veins; they are interpreted to be of hydrothermal origin. Fluorite occurs as anhedral, interstitial grains with a purple tint in plane-polarized light and 70 µm up to 1 mm across. Locally, it occurs as inclusions within biotite flakes where biotite is unaltered. This indicates that fluorite in granite porphyry of GEG has a magmatic origin and reflects high activity of fluorine in the GEG magma. Micrographic intergrowth of quartz and K-feldspar in granite porphyry is common. Commonly the contact between a granitic dyke and surrounding rhyolitic volcanic rocks is marked by quartz veins. It seems that these contacts had the role of conduits for later hydrothermal fluids from the dykes or a deeper source.

2.2 Micrographic granite

Mineralogy and appearance of micrographic granite is similar to that of microgranite porphyry, however, the former can be distinguished by lower biotite contents and finer

grain size. Its K-feldspar ($Or_{87}Ab_{13}$ to $Or_{95}Ab_5$) and plagioclase ($Ab_{90}Or_2An_8$ to $Ab_{98}An_2$) composition is similar to those in the microgranite porphyry. The intensity of micrographic growth varies. In some samples, there are discrete crystals of quartz and K-feldspar in addition to micrographic intergrowths, whereas in other samples almost all of the rock is composed of micrographic intergrowth of quartz and K-feldspar, and biotite and plagioclase are less abundant.

2.3 Aplite

Aplite at Glen Eden occurs as dykes up to 10 cm wide at a depth of ~85 m. It has granular texture and is composed of quartz, plagioclase and K-feldspar with grain size ranging from 50-400 µm, average 150 µm. No biotite or other accessory phases occur in aplite samples. Plagioclase is albitic ($Ab_{97}Or_2An_1$ to Ab_{100}) and K-feldspar (orthoclase, $Or_{86}Ab_{14}$ to $Or_{94}Ab_6$) grains are cloudy. These dykes have experienced potassic alteration and contain quartz-K-feldspar veins. The contact of aplite dykes with volcanic wall rock is sharp. Along these contacts, rhyolite groundmass has recrystallized, suggesting interaction of hot aplitic magma with cooler wall rock. Aplitic materials, in addition to aplite dykes, occur also in crenulate quartz layers and parting veins.

2.4 Crenulate quartz layers (comb layering)

Comb layering was defined by Moore and Lockwood (1973) as 'relatively unusual type of layering in granitoid rocks in which constituent crystals (plagioclase and hornblende in their study) are oriented nearly perpendicular to the planes of layering'. The types with ductile deformation are called 'crenulate quartz layers' (White et al., 1981; Kirkham and Sinclair, 1988). Comb layers are also referred to as ribbon rock, ribbon banded structures, rhythmically banded textures, brain rock, ptygmatic veins, wormy veins, vein dykes, unidirectional solidification textures and Willow Lake-type layering. Because of its deformed character, comb layering is called crenulate quartz layers, herein.

The crenulate quartz layers mainly occur within 5-10 m from the GEG dykes at depths >300 m. They are composed of quartz layers ranging in thickness from 2 mm to 3 cm. Quartz crystals in these layers are anhedral and they do not show perpendicular growth against the layer walls, possibly due to deformation and recrystallization. The quartz layers typically alternate with layers of aplitic material 1 mm to 2 cm thick. Some aplitic layers are discontinuous and terminate sharply within quartz layers. This suggests that the relative content of melt in the comb layer-forming system was low. Ptygmatic folding does not occur. Some quartz crystals in quartz layers are bent and elongate due to deformation. Similar deformation has been reported from Climax, Colorado (e.g. White et al., 1981), Hall, Nevada (Shaver, 1984a) and Anticlimax, British Colombia (Kirkham and Sinclair, 1988). Aplitic layers are composed of fine-grained quartz and feldspars, including orthoclase ($Or_{91}Ab_9$ to $Or_{97}Ab_3$) and albite ($Ab_{98}Or_1An_1$ to $Ab_{99}An_1$). Locally, quartz phenocrysts, up to 2 mm across, occur in aplitic layers. Based on microscopic and macroscopic studies, these conclusions can be made.

- The broken and bent quartz and aplite layers imply formation in a dynamic environment. Although subsequent deformation could produce partly similar features in GEG and wall rock, such features are not seen in these rocks. Also, if subsequent deformation was the main cause of bending, all layers should show this bending, whereas some of them are undeformed.

- Ductile deformation of these layers indicates that they were not completely solidified at the time of deformation. Also, deformation of some layers while the others are undeformed, suggests successive precipitation and deformation.

- The absence of a sharp boundary between quartz and aplite layers, and replacement of aplitic material by quartz suggest disequilibrium conditions during formation of quartz layering.

- The magma or fluid from which aplitic material precipitated was saturated with the components of sodic plagioclase and K-feldspar. The presence of some quartz phenocrysts in aplitic layers indicates that the magma crystallized in at least two stages, in which formation of groundmass followed crystallization of phenocrysts. The fine-grain size of aplitic material shows that the temperature difference between magma and the surrounding environment was large and magma crystallized rapidly.

- Delicate aplitic layers and close spatial relationship between crenulate quartz layers and parting veins indicate that the parent magma had very low viscosity. A similar conclusion was reached by Kirkham and Sinclair (1988).

- The low volume of aplitic materials and their mineralogical composition, which is similar to GEG, may imply that they represent a small portion of highly fractionated melt, possibly carried by escaping hydrothermal fluids. The association of aplitic material of crenulate quartz layers with quartz pods, parting veins, breccia zone and resorbed crystals suggests overlapping of magmatic processes by hydrothermal activity. Association of the crenulate quartz layers with Mo mineralization and silicification has been reported by other investigators and these layers have been considered as a prospecting guide (e.g., Povilaitis, 1978).

- The presence of primary two-phase fluid inclusions within quartz layers and quartz phenocrysts in the aplitic layers indicates the presence of hydrothermal fluid at the time of formation of these layers. Also, the similarity of formation temperature and salinity of these layers to those of other hydrothermal assemblages (Somarin and Ashley, 2004) indicates that at least the quartz layers and quartz phenocrysts in the aplitic layers have precipitated from fluid, not melt.

- Common occurrence of crenulate quartz layers in the apical parts (close to contact) of felsic intrusions related to porphyry deposits (White et al., 1981; Carten et al., 1988; Kirkham and Sinclair, 1988) may indicate that the main body of GEG is in the vicinity of these layers.

Generally there are two ideas regarding the genesis of crenulate quartz layers.

1. They have crystallized from the melt (White et al., 1981)
2. They have precipitated from the aqueous phase (Moore and Lockwood, 1973; Stewart, 1983; Shaver, 1984 a, b).

White et al. (1981) proposed that P_{H_2O} and P_{HF} increased during crystallization of the magma due to lack of hydrous minerals. The increased P_{H_2O} and P_{HF} would expand the quartz field in the ternary Q-Ab-Or system and lower the thermal minimum. They suggested that the combined effect of increasing P_{H_2O} and P_{HF} caused the precipitation of quartz without feldspar. Release of volatiles due to fracturing of wall rocks shrinks the quartz field and allows the crystallization of feldspar with quartz. This cycle occurs repeatedly to produce crenulate quartz layers. Based on this model, crenulate quartz layers have a magmatic source. It appears that even under high P_{H_2O} and P_{HF}, precipitation of pure quartz cannot be expected and some feldspar will crystallize as well. However, no feldspar

occurs in quartz layers. Furthermore, 7 to 19 wt% F is needed in the system to destabilize feldspars (Glyuk and Aufiligov, 1973). This amount of F should cause movement of the eutectic point toward the Ab apex in the Q-Ab-Or system, which is not evident in the Glen Eden Granite. Therefore, it is unlikely that the formation of crenulate quartz layers of the Glen Eden Mo-W-Sn deposit can be explained by this model.

Based on observations mentioned above, it seems that for aplitic and quartz layers, two different sources should be considered. Aplitic layers indicate evidence of crystallization from a very low-viscosity melt, whereas quartz layers have crystallized from an aqueous fluid. It is more likely that aplitic material represents the relicts or parts of the highly fractionated low-viscosity melt in a dynamic moving, mainly upward, fluid which has separated from the melt. Kirkham and Sinclair (1988) suggested that the rapid drop in fluid pressure due to brecciation and fracturing of surrounding rocks quenches the adjacent silicate melt along the roof and walls of the magma chamber. This results in the formation of aplitic or porphyritic aplitic layers between the comb quartz layers. Occurrence of this process, successively, explains the rhythmic repetition of layers. The successive brecciation at Glen Eden was able to release pressure alternately and cause upward quenching of the melt. High fluid pressure and continued movement of magma, probably, resulted in the ductile deformation of the layers (Kirkham and Sinclair, 1988). The absence of thick comb quartz layers and pegmatitic lenses may indicate trapping of a large volume of volatiles (testified by pervasive hydrothermal brecciation) and relatively rapid build-up of fluid pressure. This could prevent the growth of layer crystals before fluid escape. However, occasionally coarse-grained K-feldspar and ore minerals can be seen in the breccia pipe, indicating less rapid build-up of fluid pressure, permitting the growth of these minerals.

3. Genetic implications of micrographic texture

In the Glen Eden Granite, micrographic texture occurs as the main texture of the micrographic granite and as a texture of some phenocrysts in microgranite porphyry. Generally there are two ideas about the genesis of graphic texture.

1. Infiltration and replacement of one mineral (host) by another mineral (guest) (e.g. Augustithis, 1973).
2. Eutectic crystallization of intergrowth-forming minerals (e.g. Fenn, 1979; Kirkham and Sinclair, 1988).

Graphic textures most commonly develop in water-rich magmas, generally in the presence of a separate aqueous phase (Nabelek and Russ-Nabelek, 1990), even though studies by Fenn (1979) have shown that a separate aqueous phase is not always required. In experiments using crushed glass from bulk samples of Spruce Pine pegmatite, Burnham (1967) found that in the presence of H_2O alone, the melts crystallized to an assemblage of alkali feldspar, quartz and muscovite. However, with a solution containing 6.2 wt% total dissolved alkali feldspar, muscovite did not appear and the melt crystallized to a graphically intergrown assemblage of alkali feldspar and quartz. Based on these studies, White et al. (1981) concluded that graphic textures represent zones of accumulation of a separate, Cl-rich aqueous phase. However, the presence of F in magma, which increases the amount of water in the separate phase by decreasing its solubility in the melt, may also help the formation of graphic texture. Also, pressure-quenched crystallization is able to produce micrographic texture (Kirkham and Sinclair, 1988).

Petrographic studies show that, genetically, there are two kinds of graphic texture at Glen Eden.

1. Graphic texture in the GEG. The following observations imply that this texture is the result of eutectic crystallization rather than replacement.
    a. Absence, in fresh rocks, of replacement of other minerals, such as plagioclase, by either quartz or K-feldspar.
    b. The occurrence of micrographic granite in which the entire rock is composed of micrographic intergrowth of quartz and K-feldspar.
    c. Absence of evidence of infiltration of quartz-forming solutions and replacement of K-feldspar. Although there are some low-temperature fluid inclusions in quartz phenocrysts of GEG, there is no clear evidence of replacement of other minerals by quartz.
    d. Absence of reaction margins in host K-feldspar or other minerals.
    e. The presence of graphic grains in which K-feldspar patches occur as inclusions within quartz. In the replacement model, in which quartz has been introduced by a solution, euhedral quartz grains should have formed by progressive replacement, rather than a groundmass for K-feldspar patches (Augustithis, 1973). Furthermore there is no evidence of infiltration of K-feldspar-forming solutions into quartz grains and replacement of quartz by K-feldspar.
2. Graphic texture in potassic alteration zone. Microscopic studies show that infiltration of quartz-forming solutions into fractures, intergranular spaces and cleavages of K-feldspar resulted in the replacement of K-feldspar by quartz. This replacement looks like a graphic intergrowth and clearly is the result of post-magmatic hydrothermal activity.

It seems that the presence of crenulate quartz layers, micrographic texture and hydrothermal breccia at Glen Eden indicates saturation of magma from water and the presence of a fluid-rich environment. The presence of free vapor and aqueous phases during graphic crystallization of quartz and K-feldspar is proved by the presence of fine (2-5 μm) primary two-phase fluid inclusions within quartz of the graphic texture.

4. Emplacement of the Glen Eden Granite

The presence of topaz, fluorine-rich biotite and widespread occurrence of fluorite in all alteration assemblages indicate that the Glen Eden Granite magma was uncommonly fluorine-rich. Since fluorine has significant effects on the physico-chemical properties of granitic magma, these effects are discussed below.

4.1 Effects of fluorine on the magma

High F content of GEG and presence of magmatic fluorite provide links between this granite and other F-rich rocks, such as topaz granite, ongonites and topaz rhyolites (Kovalenko et al., 1971; Pichavant and Manning, 1984; Taylor, 1992; Kontak, 1994). The effects of fluorine in magma have been studied by many investigators. These effects can be summarized as follows.

• Fluorine decreases the solubility of water in the melt (Dingwell, 1985, 1988), so water exsolution may occur earlier during crystallization of F-rich melts (Strong, 1988). The presence of breccia pipes testifies that magma had become saturated in water and volatiles.

- Both fluorine and water lower the crystallization temperature of granitic magmas (Bailey, 1977). Manning (1981) has documented the persistence of melt at 550°C in a granite with 4% F. This effect of fluorine would allow melt to fractionate more. The occurrence of mineral deposits similar to that at Glen Eden with highly fractionated granitic rocks may suggest that this factor (more fractionation) is important for the evolution of ore-bearing vapor phase from melt, since incompatible elements, including metals, would concentrate in residual melt.
- Fluorine changes the order of crystallization by promoting quartz, topaz and feldspars above biotite (Bailey, 1977; Hannah and Stein, 1990). This could be the result of increasing the thermal stability of hydrous phases by fluorine (Hannah and Stein, 1990).
- Fluorine lowers the viscosity of melt (Dingwell et al., 1985; Hannah and Stein, 1990). At 1000°C, addition of 1 wt% F to a melt of albitic composition results in an order of magnitude decrease in melt viscosity (Dingwell, 1988). Because of the smaller temperature dependence of viscosity in F-bearing melts versus F-free melt, the effects of F on melt viscosity is greatest at 600° to 800°C (Dingwell, 1988). The lower viscosity could cause higher migration of melt and replacement into shallow levels. Approach of the melt to shallow levels in the crust and hence decreasing pressure and the escape of water and volatiles may lead to increasing viscosity. High-level emplacement of the Glen Eden Granite, along with the presence of crenulate quartz layers and parting veins indicate low viscosity of the melt.
- By decreasing the solidus temperature of the magma, the assimilation ability of the magma may be increased (Keith and Shanks, 1988).
- Due to the decreased solidification temperature of the melt, F-bearing magmas may show extreme differentiation. The solidification temperature could be as low as 550-600°C in the presence of various volatiles (Strong, 1988). The solidus of an acid melt will decrease by 60°C in the presence of a vapor phase containing 5% HF (Schroecke, 1973). The association of Sn, Mo and W ore deposits with highly fractionated granites implies that extreme differentiation is essential for the concentration of these elements in evolved aqueous phase. This explains why intrusions at high levels have more potential to associate with rare-element mineralization in comparison to those intruded at low levels, since the high-level intrusions have been differentiated more than deep-level ones (Tischendorf, 1977). Also, water saturation develops through extreme differentiation. Intrusions without high concentration of magmatic water are typically barren (Strong, 1988). So it seems that the presence of volatiles, which affect the physical and chemical properties of the magma, is crucial for the formation of rare-metal ore deposits. A strongly depolymerized F-rich melt is more capable of hosting incompatible elements than a polymerized volatile-poor melt (Webster and Holloway, 1990).
- Fluorine increases cation diffusion in silicate melts (Dingwell, 1985) which is important for the transportation of the constituents necessary for ore deposition.
- The various effects of F could cause changes in commencement of the late-magmatic metasomatic processes (Tischendorf, 1977).
- Fluorine could change the solid/melt partition coefficients of elements because the stability of each element's site within the melt is altered (Hannah and Stein, 1990).
- Fluorine increases the solubility of silicate melt in the fluid phase (Hannah and Stein, 1990).
- Fluorine increases Ab content of the near-minimum melts (Manning and Pichavant, 1988).

4.2 Emplacement of GEG

Field evidence, including presence of the breccia pipe, crenulate quartz layers and parting veins, which commonly occur in the roof of the intrusion, indicate that the Glen Eden Granite, like other leucogranites of the New England Batholith, is a high-level intrusive body. The high-level emplacement of GEG indicates that the magma was water-poor, since the main control on depth of crystallization of a rising body of granitic magma is its H_2O content (Burnham, 1979; Wyllie, 1979). Burnham (1979) pointed out that for felsic magma to attain a volcanic or sub-volcanic environment, the initial water content cannot be greater than about 3 wt%. Magma with higher initial water content would become completely crystallized after boiling of its volatiles at a depth of several kilometres (Sheppard, 1977). In addition to water, fluorine also affects the emplacement of granitic magmas. Fluorine depolymerizes the structure of the melt and decreases its viscosity which would allow higher migration and shallow-level emplacement of the magma. Also, fluorine decreases the solubility of water in the melt. This water can escape from melt as a result of pressure drop, but fluorine does not, because it enters the OH sites of biotite and possibly exists in the melt as alkali–LILE–fluoride complexes (Collins et al., 1982) or alkali-aluminium-fluoride complexes (Velde and Kushiro, 1978). Therefore, the viscosity of magma will decrease progressively while water is released, and this magma can reach epizonal environments (Plimer, 1987). The formation of massive greisen (Somarin and Ashley, 2004) before intrusion of the Glen Eden granitic dykes might be due to this released water.

The path of movement, initially, is mainly dependent on the direction of weak zones, such as faults. A velocity of 1-2 cm/year, as proposed by Bankwitz (1978), may be enough to cause upward and outward movement of melt without complete crystallization. The prolonged period of tectonic activity in the New England area during Permo-Triassic compression and extension (Collins et al., 1993) could produce suitable structures, such as faults, for the rise of plutons. Also, fracturing of roof rocks by heat flow from the melt, which increases the amount of elastic energy, helps the movement of the melt (Bankwitz, 1978). As mentioned above, high content of F would retard crystallization of melt and allow it to move away from the magma chamber. The intense veining of parts of GEG, while the other parts show less or no veining, may reflect that the outer vein-bearing parts became colder than inner parts due to encountering cold wall rock.

The intrusive body utilizes structures which are later utilized by metal-bearing hydrothermal fluids (Plimer and Kleeman, 1985). The presence of quartz veins at boundaries between granitic dykes and wall rock at Glen Eden supports this idea and indicates that these boundaries were relatively weak zones, along which hydrothermal fluids could easily move.

On the whole, the high-level emplacement of the GEG and its highly differentiated character reflect high content of fluorine in the magma. Phosphorus, like F, also decreases the liquidus and solidus temperatures of the melt by modifying the silica network with the formation of phosphate-oxygen-metal complexes (London, 1987; Hannah and Stein, 1990). However, the low concentration of P in the GEG and absence of apatite in the hydrothermal assemblages indicate low P content of magma.

5. Geochemistry

5.1 Major element geochemistry

The Glen Eden Granite is highly felsic, as indicated by SiO_2 contents between 76 and 78 percent (Table 1). Aplite samples show potassic alteration. The chemical compositions of

	Granite porphyry										Micrographic granite			
	R75283	R75284	R75285	R75286	R75287	R75288	R75289	R75290	R75291	**Average**	R75292	R75293	R75294	**Average**
SiO_2	76.27	76.24	76.97	76.33	76.77	77.60	76.70	76.12	77.23	**76.69**	76.66	77.78	77.72	**77.39**
TiO_2	0.06	0.07	0.08	0.06	0.05	0.09	0.05	0.06	0.05	**0.06**	0.10	0.06	0.04	**0.07**
Al_2O_3	12.82	12.34	12.15	13.04	13.15	12.63	12.66	12.43	12.39	**12.62**	12.53	12.29	12.34	**12.39**
Fe_2O_3	0.11	0.18	0.30	0.13	0.08	0.10	0.17	0.18	0.16	**0.16**	0.25	0.08	0.06	**0.13**
FeO	0.43	0.82	0.70	0.38	0.21	0.22	0.60	0.63	0.55	**0.50**	0.71	0.48	0.63	**0.61**
MnO	0.02	0.03	0.03	0.02	0.01	0.01	0.03	0.03	0.02	**0.02**	0.03	0.02	0.03	**0.03**
MgO	0.12	0.04	0.06	0.08	0.07	0.08	0.05	0.05	0.04	**0.06**	0.06	0.07	0.10	**0.08**
CaO	0.27	0.33	0.40	0.26	0.20	0.23	0.31	0.35	0.39	**0.30**	0.43	0.38	0.36	**0.39**
Na_2O	2.78	3.17	3.67	3.05	3.22	3.04	3.58	3.46	3.71	**3.30**	3.86	3.45	2.94	**3.42**
K_2O	5.25	5.29	4.56	5.94	5.43	4.83	4.54	4.96	4.70	**5.05**	4.32	4.17	4.20	**4.23**
P_2O_5	0.01	0.01	0.01	0.01	0.01	0.01	0.01	0.01	0.01	**0.01**	0.01	0.00	0.02	**0.01**
S	0.03	0.01	0.01	0.02	0.02	0.02	0.05	0.01	0.01	**0.02**	0.01	0.02	0.02	**0.02**
LOI	1.01	1.40	0.54	0.70	0.54	0.84	0.92	0.78	0.53	**0.81**	0.54	0.87	1.33	**0.91**
Total	99.15	99.92	99.47	100.00	99.74	99.68	99.62	99.06	99.78	**99.58**	99.50	99.65	99.77	**99.66**
$K_2O/$ Na_2O	1.89	1.67	1.24	1.95	1.69	1.59	1.27	1.43	1.27	**1.53**	1.12	1.21	1.43	**1.24**
Q	39.02	36.25	36.83	34.97	36.66	40.81	37.47	35.82	36.45	**37.14**	36.24	40.52	43.20	**39.99**
C	2.10	0.82	0.47	1.14	1.63	2.01	1.33	0.77	0.52	**1.20**	0.73	1.42	2.34	**1.50**
Or	31.03	31.27	26.95	35.11	32.09	28.55	26.80	29.32	27.75	**29.87**	25.53	24.65	24.82	**25.00**
Ab	23.52	26.78	31.05	25.81	27.25	25.68	30.25	29.24	31.39	**27.89**	32.66	29.19	24.88	**28.91**
An	1.27	1.60	1.92	1.22	0.93	1.08	1.45	1.65	1.88	**1.44**	2.10	1.86	1.66	**1.87**
Di	0.00	0.00	0.00	0.00	0.00	0.00	0.00	0.00	0.00	**0.00**	0.00	0.00	0.00	**0.00**
Hy	0.86	1.38	1.06	0.70	0.38	0.35	0.95	1.07	0.89	**0.85**	1.11	0.89	1.30	**1.10**
Mt	0.16	0.26	0.43	0.19	0.12	0.14	0.25	0.23	0.26	**0.23**	0.36	0.12	0.09	**0.19**
Ilm	0.10	0.12	0.14	0.10	0.09	0.16	0.09	0.10	0.09	**0.11**	0.19	0.11	0.08	**0.13**
Ap	0.02	0.01	0.02	0.02	0.02	0.02	0.02	0.02	0.01	**0.02**	0.01	0.00	0.05	**0.02**
Py	0.06	0.02	0.02	0.03	0.04	0.04	0.09	0.02	0.02	**0.04**	0.02	0.04	0.04	**0.03**
Total	98.15	98.51	98.92	99.30	99.21	98.84	98.71	98.24	99.26	**98.79**	98.96	98.79	98.45	**98.73**
Ab/ An	18.52	16.74	16.17	21.16	29.30	23.78	20.86	17.72	16.70	**19.37**	15.55	15.69	14.99	**15.46**
100Mg /Mg+Fe	40	9	16	34	49	61	16	13	14	**23**	17	24	24	**22**
A.S.	1.19	1.07	1.04	1.09	1.14	1.19	1.12	1.06	1.04	**1.10**	1.06	1.13	1.23	**1.14**
DI	94	94	95	96	96	95	95	94	96	**95**	94	94	93	**94**

Table 1. Major element analyses and CIPW norms of the Glen Eden Granite, compared with average calc-alkaline and alkaline granites of Nockolds (1954), and average granite of Le Maitre (1976) and average I-, S-, and A-type granites of Whalen et al. (1987) and biotite porphyry of Climax (White et al., 1981).

	1	2	3	4	5	6	7
SiO_2	75.70	72.08	73.86	72.04	73.39	73.39	73.81
TiO_2	0.56	0.37	0.20	0.30	0.26	0.28	0.26
Al_2O_3	12.70	13.86	13.75	14.42	13.43	13.45	12.40
Fe_2O_3	0.47	0.86	0.78	1.22	0.60	0.36	1.24
FeO	0.57	1.67	1.13	1.68	1.32	1.73	1.58
MnO	NA	0.06	0.05	NA	0.05	0.04	0.06
MgO	0.37	0.52	0.26	0.71	0.55	0.58	0.20
CaO	1.07	1.33	0.72	1.82	1.71	1.28	0.75
Na_2O	3.10	3.08	3.51	3.69	3.33	2.81	4.07
K_2O	5.60	5.46	5.13	4.12	4.13	4.56	4.65
P_2O_5	ND	ND	ND	ND	0.07	0.14	0.04
S	ND	ND	ND	ND	ND	ND	ND
LOI	ND	ND	ND	ND	ND	ND	ND
Total	100.14	99.29	99.39	100.00	98.84	98.62	99.06
K_2O/Na_2O	1.81	1.77	1.46	1.12	1.24	1.62	1.14
Q	33.63	28.80	31.34	29.13	33.20	35.24	30.19
C	0.00	0.46	1.11	0.58	0.54	1.90	0.00
Or	33.10	32.27	30.32	24.35	24.41	26.95	27.48
Ab	26.23	26.06	29.69	31.22	28.18	23.78	34.44
An	4.20	6.60	3.57	9.03	8.03	5.44	1.83
Di	0.87	0.00	0.00	0.00	0.00	0.00	1.40
Hy	0.52	3.15	1.84	3.35	2.96	3.94	1.34
Mt	0.21	1.25	1.13	1.77	0.87	0.52	1.80
Ilm	1.06	0.70	0.38	0.57	0.49	0.53	0.49
Ap	0.00	0.00	0.00	0.00	0.17	0.33	0.09
Py	0.00	0.00	0.00	0.00	0.00	0.00	0.00
Total	100.14	99.29	99.39	100.00	98.84	98.62	99.06
Ab/An	6.25	3.95	8.32	3.46	3.51	4.37	18.82
100Mg/Mg+Fe	100	48	42	60	53	43	30
A.S.	0.97	1.03	1.09	1.04	1.03	1.13	0.95
DI	93	87	91	85	86	86	92

NA = Not analyzed   DI = Differentiation index
ND = No data   LOI = Loss on ignition
A.S. = Degree of aluminum saturation (molecular proportion of $Al_2O_3/CaO+Na_2O+K_2O$)

1) Biotite porphyry-Climax (White et al., 1981)	5) Average of felsic I-type granites (Whalen et al., 1987)
2) Average of calk-alkaline granite (Nockolds, 1954)	6) Average of felsic S-type granites (Whalen et al., 1987)
3) Average of alkali granite (Nockolds, 1954)	7) Average of A-type granites (Whalen et al., 1987)
4) Average of granite recalculated to 100% (Le Maitre, 1976)	

Cont. Table 1.

	Granite Porphyry										Micrographic Granite						
	R752 83	R752 84	R752 85	R752 86	R752 87	R752 88	R752 89	R752 90	R752 91	**Aver age**	R752 92	R752 93	R752 94	**Aver age**	1	2	3
Nb	27	40	27	26	38	26	42	41	36	**34**	28	23	13	**21**	12	13	37
Zr	90	103	96	89	113	115	126	110	96	**104**	107	86	81	**91**	144	136	528
Y	54	83	76	58	58	66	114	106	109	**80**	79	83	87	**83**	34	33	75
Sr	11	3	4	17	3	4	3	6	5	**6**	5	5	17	**9**	143	81	48
Rb	488	510	365	552	434	408	309	458	427	**439**	379	324	321	**341**	194	277	169
Th	50	53	48	44	50	52	52	50	48	**50**	50	46	44	**47**	22	18	23
Pb	37	38	33	43	43	38	38	36	39	**38**	35	36	22	**31**	23	28	24
As	2	4	5	3	4	8	3	2	8	**4**	5	5	5	**5**	ND	ND	ND
U	9	14	15	12	11	12	12	12	17	**13**	17	11	7	**12**	5	6	5
Ga	24	25	21	23	25	25	24	27	26	**24**	21	25	20	**22**	16	17	25
Zn	5	17	47	6	3	7	26	8	8	**14**	25	13	19	**19**	35	44	120
Cu	5	8	3	<2	<2	<2	<2	<2	<2	**3**	<2	2	3	**2**	4	4	2
Ni	20	18	6	3	3	25	10	19	11	**13**	4	2	7	**4**	2	4	<1
Ce	38	29	51	39	40	41	43	34	37	**39**	58	50	62	**57**	68	53	137
Nd	21	18	22	22	26	21	24	24	23	**22**	28	34	38	**33**	ND	ND	ND
Ba	38	19	10	105	20	16	15	16	10	**28**	31	19	42	**31**	510	388	352
V	<2	2	4	5	<2	<2	3	5	<2	**3**	<2	<2	4	**3**	22	23	6
La	16	12	18	19	15	13	13	18	10	**15**	25	16	22	**21**	ND	ND	ND
Sc	<2	4	6	6	<2	6	<2	7	3	**4**	8	4	5	**6**	8	8	4
Sn	<3	4	3	<3	<3	<3	<3	<3	<3	**<3**	3	5	3	**4**	ND	ND	ND
Mo	1	2	10	5	2	2	1	2	1	**3**	2	1	2	**2**	ND	ND	ND
W	10	65	18	286	17	16	21	32	24	**54**	12	14	8	**11**	ND	ND	ND
F	NA	1580	1530	NA	1180	480	NA	1430	NA	**1240**	3200	3400	<250 0		ND	ND	ND
K/Rb	89	86	104	89	104	98	122	90	91	**96**	95	107	109	**103**	177	137	229
Rb/ Sr	44	170	91	32	145	102	103	76	85	**71**	76	65	19	**38**	1.36	3.42	3.52
Rb/ Ba	13	27	37	5	22	26	21	29	43	**16**	12	17	8	**11**	0.38	0.71	0.48
Ga/ Al	3.54	3.83	3.27	3.34	3.59	3.74	3.59	4.11	3.97	**3.66**	3.17	3.85	3.07	**3.36**	2.25	2.39	3.75

NA = Not analyzed	ND = No data	
1) Average Felsic I-type (Whalen et al. 1987)	2) Average Felsic S-type (Whalen et al. 1987)	3) Average A-type (Whalen et al. 1987)

Table 2. Trace element abundances in the Glen Eden Granite and average I-, S-, and A-type granites of Whalen et al. (1987). F values of less than 2500 ppm are from sodium peroxide fusion/SIE method whereas values shown by <2500 ppm (less than detection limit) are from XRF.

microgranite porphyry and micrographic granite are similar, however micrographic granite has lower K_2O and higher F, Nd and, in some samples, Ce (Table 2). The characteristics of GEG are similar to granites associated with Climax-type molybdenum ore deposits (White et al., 1981). The GEG, like Climax-type rocks, shows enrichment in silica and depletion in Ca, Al, total Fe, and Mg with respect to both the average calc-alkaline and alkaline granites of Nockolds (1954). Average K_2O/Na_2O in microgranite porphyry is close to that of average alkaline granite (Nockolds, 1954) and average normal granite (Le Maitre, 1976), but this ratio in micrographic granite is less than that of alkaline granite and is more than the average of normal granite. Normative Ab/An ratio is high and reflects the low Ca content of the GEG.

The samples of microgranite porphyry and micrographic granite show little chemical variation and no clear trends on Harker-type diagrams using SiO_2 or MgO as an index of possible fractionation (Fig. 2). Although the least-altered samples were chosen for analysis,
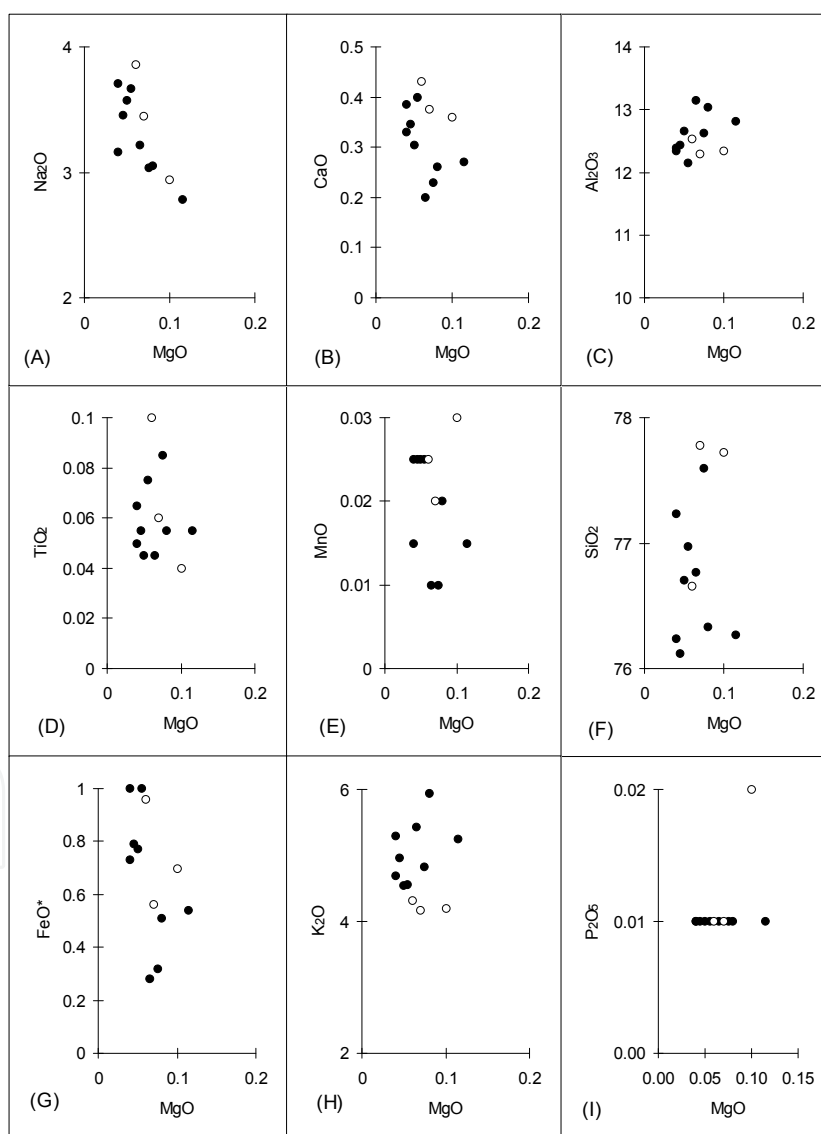
Fig. 2. Chemical variation diagrams for major elements of the GEG. None of these elements defines a well-developed trend. All oxides are in percent. Open circle = micrographic granite, closed circle = granite porphyry.

some scattering in Harker diagrams may be due to slight hydrothermal alteration. However, one of the features of Climax-type rocks is that almost none of them has completely escaped interaction with hydrothermal fluids (White et al., 1981). The GEG contains very low concentrations of P_2O_5 and CaO. Although low concentrations of CaO, Sr and Ba (Table 2) may be due to post-magmatic hydrothermal alteration, it seems that they reflect strong fractionation of the GEG magma. The geochemical changes accompanying progressive fractionation include enrichment of melt in alkali elements (Fig. 3A).
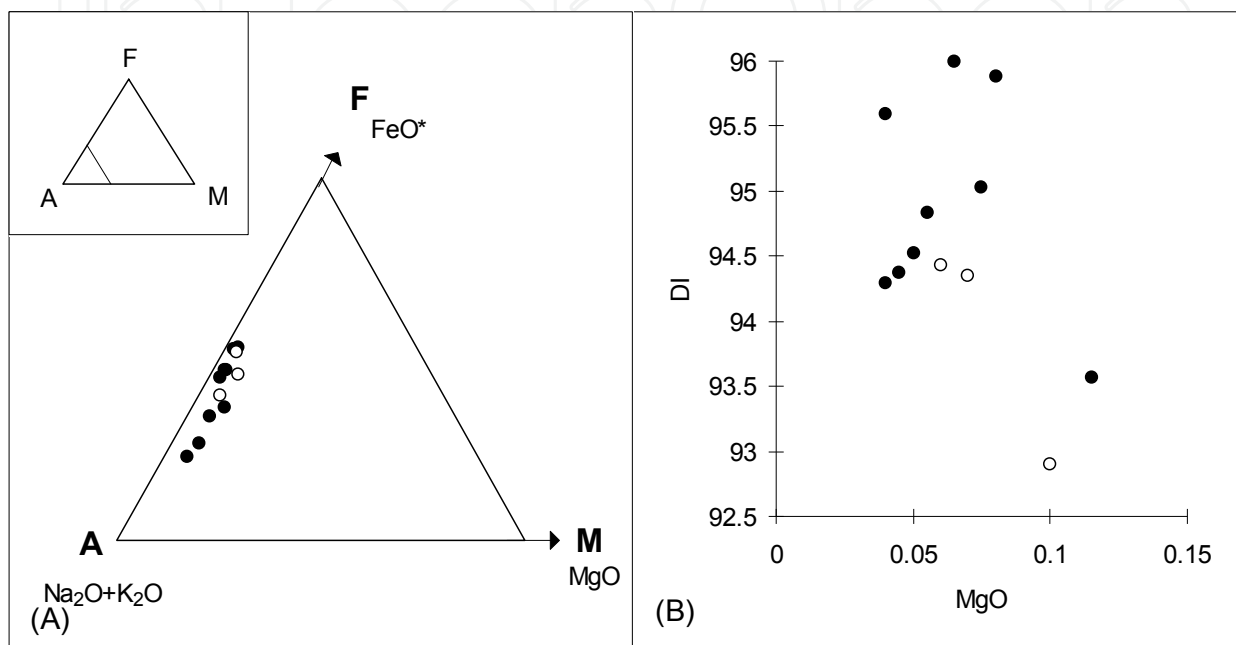
Fig. 3. A - FeO* - Na_2O+K_2O - MgO diagram for GEG samples showing evolution of the GEG toward the alkali apex. B - Plot of DI versus MgO for GEG samples showing no clear trend. All oxides are in percent. Open circle = micrographic granite, closed circle = granite porphyry.

Differentiation indices (DI= normative quartz + albite + orthoclase) for the GEG range from 93 to 97 (Table 1) which is like that of Climax granite (91-94, White et al., 1981). Inasmuch as the differentiation index represents the degree of magmatic evolution, and the normative constituents considered represent minerals with low entropies of melting (Carmichael et al., 1974; White et al., 1981), the high differentiation indices of the GEG suggest crystallization from highly differentiated, low-temperature melts. Like major elements, DI does not show any definite trend when plotted against MgO (Fig. 3B). Although the GEG, like Climax-type granites (White et al., 1981), is alkali rich, its molecular proportion of Al_2O_3 is a little more than its molecular proportion of $CaO+Na_2O+K_2O$, and so it is corundum normative (Table 1). Thus GEG is Al-saturated rather than peralkaline, like other Climax-type rocks (White et al., 1981). The GEG has peraluminous nature, however the samples show a trend toward the peralkaline field (Fig. 4A). This along with trends in Fig. 4B-C suggests that with increasing fractionation (i.e. decreasing MgO) peralkalinity increases and peraluminousity decreases. This trend (enrichment in alkali elements with fractionation), also can be seen in Fig. 3A.

A low initial H_2O content for the GEG magma can be inferred from the high-level emplacement of this granite. Furthermore, chemical composition of the GEG shows low

CaO, FeO and MgO contents of the magma. Under these conditions, high fluorine contents would not crystallize as fluorite nor substitute in the structure of ferromagnesian minerals, such as biotite. This would indicate that extreme enrichment in F (>4%) and Cl (>5000 ppm) could occur in the magma and in associated hydrothermal fluids during the late stages of the crystallization of the magma (Hannah and Stein, 1990; Webster and Holloway, 1990).
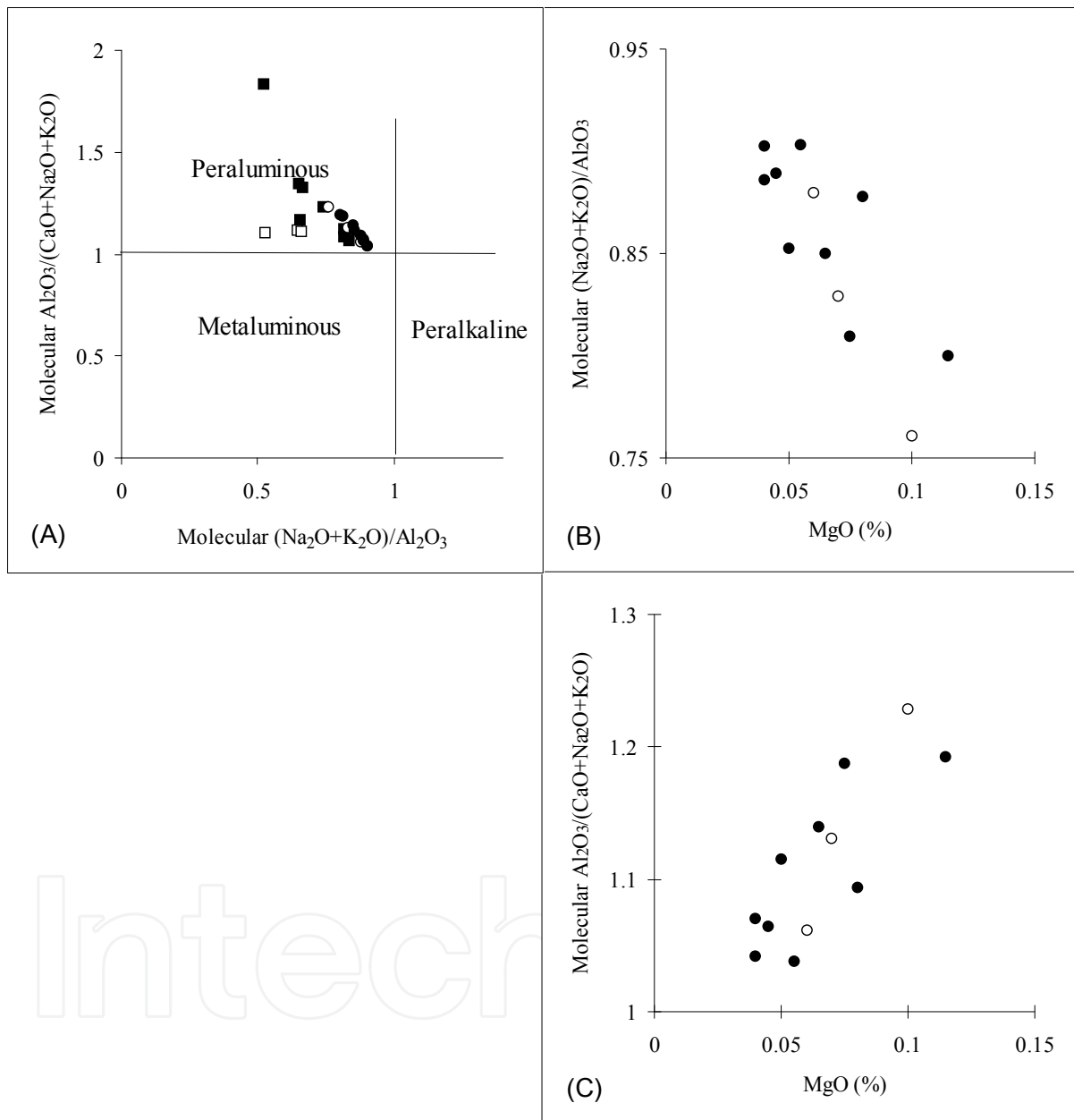

Fig. 4. A- Plot of peraluminousity index (molecular $Al_2O_3/(CaO+Na_2O+K_2O)$) versus peralkalinity index (molecular $(Na_2O+K_2O)/Al_2O_3$) for the GEG and volcanics samples showing peraluminous nature of these rocks. B- Plot of peralkalinity index versus MgO showing increasing peralkalinity with fractionation. C- Plot of peraluminousity index versus MgO showing decreasing peraluminousity with fractionation. Closed circle = granite porphyry, open circle = micrographic granite, closed square = rhyolite, open square = dacite and rhyodacite (date for volcanic rocks from Somarin, 1999).

5.2 Trace element geochemistry

Trace element abundances in GEG are presented in Table 2. Some trace elements such as Nb, Y, Ga, Zr, U, Nd, La and Ce show poorly developed trends in Harker-type diagrams (Fig. 5).
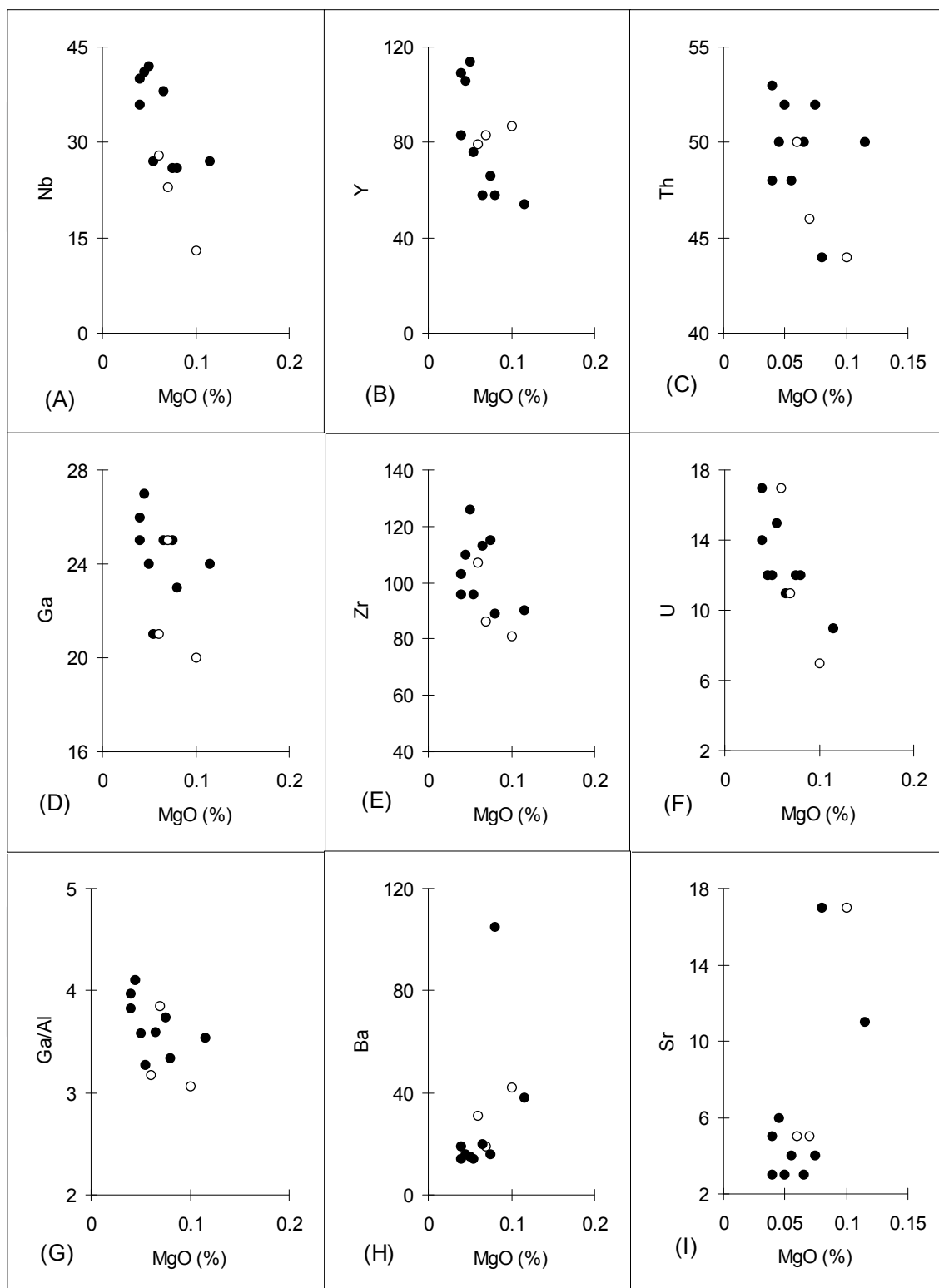
Fig. 5. Chemical variation diagrams for trace elements (in ppm) of the GEG. Open circle = micrographic granite, closed circle = granite porphyry.
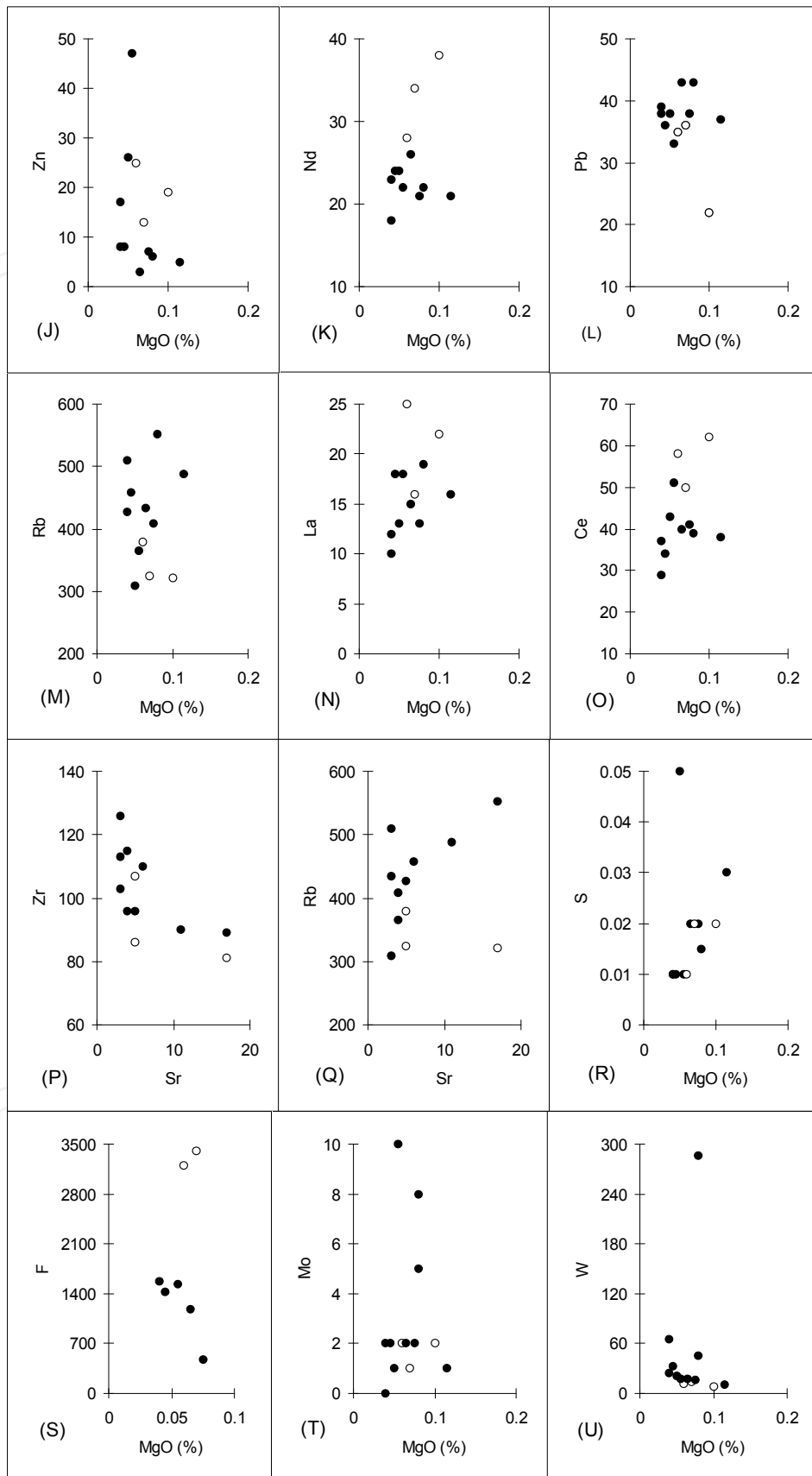
Cont. Fig. 5.

However, due to narrow range and low concentrations (near detection limit) of MgO, these trends may not be significant. The important trace element features of the GEG are low concentrations of Sr, Ba, Zr and Zn and high concentrations of Y, Th, U, and Ga relative to average A-type, felsic I- and S-type granites. Also GEG contains high concentrations of F and W, similar to other ore-associated granites (Tischendorf, 1977). High values and wide ranges of Rb/Ba (5 to 43) and Rb/Sr (18 to 170) in microgranite porphyry and micrographic granite indicate crystal fractionation in the magma (Chappell and White, 1992). High Rb/Sr (commonly over 25), very low CaO (<0.7%) and pronounced Eu anomalies (<0.3) are characteristics of granitoids associated with Sn and W ore deposits (Stemprok, 1990). Fluorine has the highest enrichment in micrographic granite (Fig. 5S). The high F concentrations in the GEG and micas (Somarin and Ashley, 2004) resemble those of topaz granites, topaz rhyolites, ongonites and other volatile-enriched granitic rocks (see Manning and Pichavant, 1988). It is suggested that strong fractionation in the melt caused extraction of metal-bearing fluid from the parent magma. GEG contains high W concentrations and it is possible that sub-solidus leaching of this granite could provide additional W for mineralization. However, the volcanic wall rocks have low concentrations of Mo, W and Sn (Somarin and Ashley, 2004) and could not be a major source of these metals.

5.3 Glen Eden Granite in the Q-Or-Ab system

Average normative Q:Ab:Or in microgranite porphyry is Q_{39}, Ab_{29}, Or_{32} and in micrographic granite is Q_{42}, Ab_{31}, Or_{27}. These approximate the eutectic composition Q_{39}, Ab_{30}, Or_{31} for the calcium-poor granite system at P_{H_2O} =0.5 kbar (Winkler, 1974). Holtz et al. (1992) showed that decreasing H_2O content of the melt causes a rise in liquidus temperatures and a progressive shift of minimum and eutectic compositions toward the Q-Or join at approximately constant normative quartz content. The GEG does not show such shift.

Microgranite porphyry and micrographic granite samples plot around the minimum melt composition on the Q-Or-Ab ternary diagram for F-poor Q-Or-Ab-H_2O systems, whereas aplite samples plot toward the Or apex, reflecting the potassic alteration of these samples (Fig. 6). The minimum melt composition of these samples explains the absence of well-defined trends in Harker diagrams. The samples do not have Ab-enriched compositions expected of near-minimum melts in F-rich Q-Or-Ab-H_2O systems (Fig. 6A) (Manning and Pichavant, 1988), but this does not necessarily prove that the GEG melt was F-poor. There is a possibility that the GEG was a minimum melt at P less than 1 kbar but with higher concentrations of fluorine. However, in a calcium-poor granite system, like GEG, with Ab/An >15, as little as 0.5% fluorine in the melt could significantly affect the crystallization processes, since crystallization of fluorite will not occur until the late stages.

The pattern of data in the Q-Or-Ab system in the GEG is very similar to that of East Kemptville, Nova Scotia, in which data points plot around the minimum in the F-poor system, suggesting F concentration of less than 1% in the melt, while the effects of F in the various geochemical trends and greisen formation are clear (Richardson et al., 1990). The large amount of F as topaz and fluorite which accompany all the alteration assemblages in the Glen Eden Mo-W-Sn deposit and the presence of primary magmatic fluorite and F-rich biotite in this granite indicate the presence of F in the magma and its effects on the magmatic differentiation of GEG. F-rich granitic rocks typically contain between 0.5 and 2.5 wt% F (Keppler, 1993). F contents measured in granitic rocks should be considered as lower limits for the original F contents of the respective melts as large amounts of F could have been lost

by the evolution of a fluid phase (Keppler, 1993). In the Glen Eden prospect, the widespread occurrence of fluorite in all assemblages indicates that a large amount of F has been concentrated in the late-stage fluids.

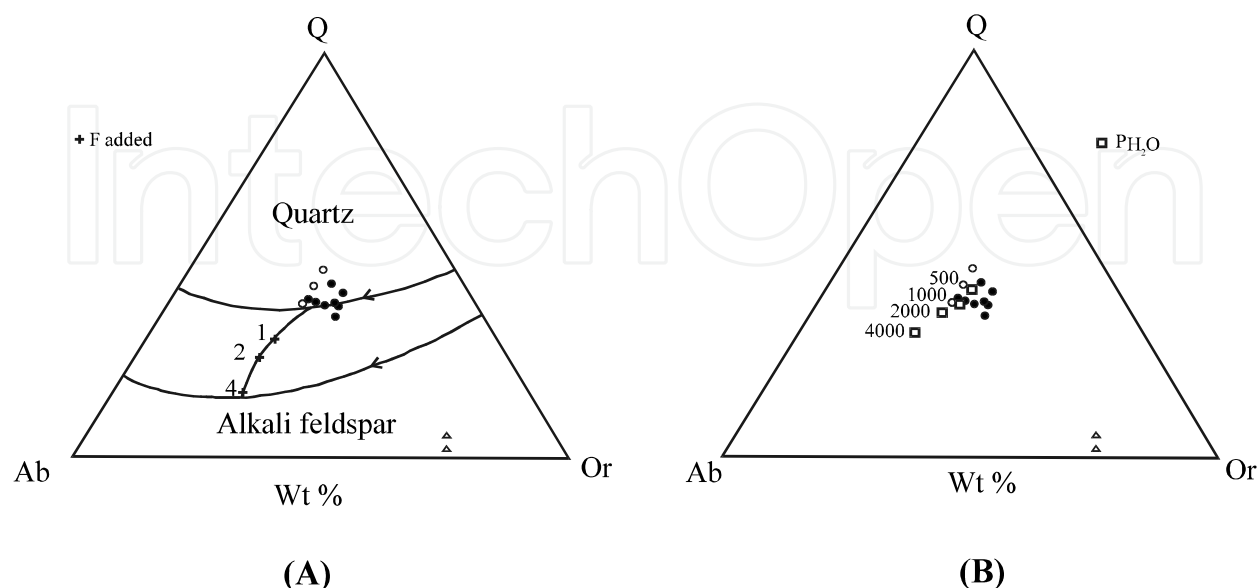**(A)**   **(B)**

Fig. 6. A- The GEG compositions (triangle = aplite, open circle = micrographic granite, closed circle = granite porphyry) compared with liquidus phase relationships in the system Q-Ab-Or at 1 kbar total pressure with excess water (Tuttle and Bowen, 1958) and with F added (in %) under water-saturated conditions (after Manning and Pichavant, 1988). B- Position of minima and eutectics in the system Q-Ab-Or at various P_{H_2O} (Tuttle and Bowen, 1958; Luth, 1976). H_2O pressures are given in bars.

Crystallization of GEG has probably occurred between 500 and 1000 bars (Fig. 6B) which suggests high-level emplacement of the GEG. Also, compositional uniformity of analyzed granite samples and their similarity to minimum melt composition at low P_{H_2O} may imply that at least this part of the GEG has crystallized under low P_{H_2O}, since with increasing P_{H_2O} there is more potential for differentiation. This may suggest that these dykes have crystallized after separation and escape of the first episode of aqueous phase. The absence from the GEG of older hydrothermal alterations, which are recognized in the volcanic wall rock, supports this idea and indicates that there was an activation of the still-unsolidified magma chamber which yielded the emplacement of granitic and aplitic dykes within the alteration products. These observations do not imply that water content of the melt was low, since the presence of breccia pipe and the great quantity of hydrothermal veins and assemblages in the central zone reflects a high content of water.

6. Classification of the Glen Eden granite

It seems that three factors have influenced the concentrations of major and trace elements in the GEG.

1. The composition of the protolith: High concentrations of elements such as Th and U, which are high not only in the GEG but also in other I-type leucogranites of the New England area [e.g. Gilgai (Walsh, 1991; Stroud, 1995; Vickery et al., 1997), Kingsgate and

Mount Jonblee (Plimer, 1973), Stanthorpe (Bampton, 1988), Mole (Brodie, 1983; Stegman, 1983; Kleeman, 1985; Vickery et al., 1997), Dumboy-Gragin (Vickery et al., 1997) and Oban River (Le Messurier, 1983)] most probably reflect the composition of the protolith.

2. Post-magmatic hydrothermal alteration: The concentrations of CaO, Sr and possibly Ba are less than those that can be attained by fractional crystallization alone and it seems that destruction of feldspars by hydrothermal solutions can account for their low concentrations. Since P_2O_5 is more immobile than those components mentioned above, it seems that the low concentrations of P_2O_5 are unlikely to be the result of hydrothermal leaching.

3. Fractionation in the melt: It seems that fractionation was the most important factor controlling the composition of the GEG. Almost all of the geochemical characteristics of the GEG, such as high SiO_2, Rb, U, Th, Nb, Y, Ga and W and low concentrations of CaO, P_2O_5, Ba, Sr, Zr and Zn and high values and wide ranges of Rb/Ba and Rb/Sr can be explained by various degrees of fractionation of the magma.

Comparison of the GEG with well-known I-, S- and A-type granites is complicated since various investigators have reported different average values for some elements and other features of these granites (e.g. Whalen et al, 1987; Chappell and White, 1992). For example DI of the GEG resembles that of average A-type granite of Whalen et al. (1987) (Table 1), but is more similar to that of average fractionated I-type granite of Chappell and White (1992) (Table 3). The problem of determining I-, S- or A-type affinities of highly felsic granites (such as GEG) has been addressed by several authors (e.g., Whalen et al., 1987; Eby, 1990; Chappell and White, 1992). Aluminium saturation index (ASI; Zen, 1986), molecular $Al_2O_3/(Na_2O+K_2O+CaO)$, in the GEG varies between 1 and 1.2. Avila-Salinas (1990) used ASI=1.1 as a boundary between I- and S-type granites. Chappell and White (1992) showed that ASI in S-type granites of Lachlan Fold Belt (LFB), Australia, are always greater than 1 whereas I-type granites generally show ASI<1.1, although 2.8% of them have ASI>1.1. They explained higher ASI in S-types to be a reflection of sedimentary source rocks which contain more clay and so more Al. In contrast, lower ASI in I-types results from lower Al contents in igneous sources. However, they suggested that compositionally very similar felsic granites can be produced from these two quite different source rocks. In such circumstances, the only clue to the nature of a granite protolith might well be isotopic compositions (Chappell and White, 1992). Non-diagnostic values of ASI in the GEG and the very felsic composition of this granite may suggest that it cannot be classified on this criterion alone, and also no conclusion can be made about the source rocks, without isotopic data. Low concentrations of CaO and Sr and resultant higher values of ASI in the GEG may partly reflect slight leaching of these elements by hydrothermal solutions.

The average compositions of microgranite porphyry and micrographic granite are compared, in Table 3, with the average compositions of unfractionated and fractionated felsic I- and S-type granites and A-type granites (data from Chappell and White, 1992). As can be seen, GEG in both major and trace elements is mainly similar to fractionated I- and A-type granites. However, in some elements, GEG shows similarity to other types as well. GEG has very low concentrations of Fe_2O_3 in comparison with others, which indicates the reduced character of this granite. K_2O concentrations of the GEG overlap all types of granites. CaO, Sr and Ba concentrations are more similar to fractionated I-type, but actually

Average GEG (porphyry)	Average GEG (micro-graphic)	Unfracti-onated I-type	Fracti-onated I-type	Unfracti-onated S-type	Fracti-onated S-type	A-type	Similar type
SiO_2 76.69	77.39	72.90	76.17	71.58	74.40	73.47	FI
TiO_2 0.06	0.07	0.30	0.10	0.42	0.16	0.30	FI
Al_2O_3 12.62	12.39	13.48	12.51	13.83	13.50	12.88	FI, A
Fe_2O_3 0.16	0.13	0.54	0.32	0.45	0.28	0.90	?
FeO 0.50	0.61	1.47	0.71	2.38	1.14	1.63	FI
MnO 0.02	0.03	0.05	0.04	0.05	0.04	0.06	FI, FS
MgO 0.06	0.08	0.66	0.12	1.02	0.27	0.30	FI
CaO 0.30	0.39	1.63	0.61	1.74	0.67	1.06	FI
Na_2O 3.30	3.42	3.27	3.37	2.57	3.06	3.50	UI, FI, A
K_2O 5.05	4.23	4.42	4.92	4.33	4.84	4.62	?
P_2O_5 0.01	0.01	0.09	0.02	0.14	0.18	0.07	FI
FeO* 0.64	0.73	1.96	1.00	2.79	1.39	2.44	FI
Nb 34	21	14	21	12	19	26	FI, A
Zr 104	91	151	116	168	92	322	FS
Y 80	83	38	75	34	28	71	FI, A
Sr 6	9	147	31	114	43	96	FI
Rb 439	341	219	424	221	475	188	FI, FS
Th 50	47	25	47	19	17	24	FI
Pb 38	31	29	35	28	25	27	?
U 13	12	6	16	4	11	5	FS
Ga 24	22	16	19	17	21	22	A
Zn 14	19	38	29	53	46	95	FI
Cu 3	2	6	2	7	3	5	FI, A
Ni 13	4	5	<1	10	2	2	UI, US, FS,A
Ce 39	57	74	79	63	37	130	US, FS
Ba 28	31	488	99	512	150	547	FI
V 3	3	25	3	41	7	9	FI
La 15	21	35	35	28	16	55	FS
Sc 4	6	8	6	10	5	11	FI, FS
Sn <3	4	7	13	8	23	8	?
Mo 3	2						
W 54	11						
F 1240							
As 4	5						
Nd 22	33						
S (%) 0.02	0.02						
Q 37.00	40.00	31.89	35.87	33.65	35.98	32.06	FI, FS
Or 30.00	25.00	26.12	29.08	25.59	28.61	27.31	?
Ab 28.00	29.00	27.67	28.52	21.75	25.89	29.62	UI, FI, A
An 1.44	1.87	7.50	2.90	7.72	2.15	4.80	FS
Hy 0.85	1.10	3.49	1.25	5.94	2.34	2.61	FI
Mt 0.23	0.19	0.78	0.46	0.65	0.41	1.30	?
Ilm 0.11	0.13	0.57	0.19	0.80	0.30	0.57	FI

Ap	0.02	0.02	0.21	0.05	0.33	0.42	0.17	FI
C	1.20	1.50	0.57	0.58	2.09	2.44	0.36	?
Py	0.04	0.03						
DI	95	94	86	93	81	90	89	FI
ASI	1.10	1.14	1.03	1.04	1.15	1.17	1.02	?
$100Mg/Mg+Fe$	23	22	54	29	50	35	34	FI
K_2O/Na_2O	1.53	1.24	1.35	1.46	1.68	1.58	1.32	?
Rb/Sr	71	38	1.50	14	2	11	2	FI
Rb/Ba	16	11	0.50	4.30	0.40	3	0.30	FI
$10000*Ga/Al$	3.66	3.36	2.24	2.87	2.32	2.93	3.22	A

*Total Fe as FeO, FI= Fractionated I-type, FS= Fractionated S-type, A= A-type, UI= Unfractionated I-type, US= Unfractionated S-type.

Table 3. Comparison of the GEG with average compositions of various types of granites (data from Chappell and White, 1992).

they are very low in GEG due to hydrothermal leaching. A-type granites have higher Nb, Y, La, Ce, Sc, Zn, Zr and Ga in comparison to all I- and S-types. However, for Nb and Ga, the fractionated I- and S-type averages move towards the A-type values, relative to unfractionated values, as also does Y for the I-types (Chappell and White, 1992). These changes due to fractionation also increase Rb, U and Sn and decrease Ba and Sr concentrations in fractionated I- and S-types relative to A-types. It seems that increasing Ga and decreasing Al in fractionated granites, especially in fractionated I-types which contain less Al_2O_3, would cause highly fractionated granites to plot in the A-type field in discrimination diagrams of Whalen et al. (1987). Whalen et al. (1987) showed that A-type granites have a high ratio of 10000Ga/Al (>2.6) and they used this ratio for the construction of discrimination diagrams. On these diagrams, high concentrations of Ga and resultant high Ga/Al ratios cause the GEG to plot within the A-type granite field (Fig. 7). However,Whalen et al. (1987) stated that highly fractionated felsic I- and S-type granites can have high Ga/Al ratios and overlap with A-types. They suggested that these fractionated rocks can be distinguished from A-types using Zr+Nb+Ce+Y as a discriminator. Use of this discriminator is based on the principle that at any given degree of fractionation, the A-type granites would contain higher abundances of these elements. On the FeO_{total}/MgO versus Zr+Nb+Ce+Y diagram, GEG plots in all fields. This may be due to post-magmatic alteration. On the K_2O+Na_2O/CaO versus Zr+Nb+Ce+Y diagram of Whalen et al. (1987), FeO_{total}/MgO versus SiO_2 and 10000Ga/Al versus Zr+Nb+Ce+Y diagrams of Eby (1990) (Fig. 8), who used a higher minimum Ga/Al ratio for A-type granites, GEG samples plot in both 'Fractionated Granite' and A-type granite fields. In the multicationic diagram of Batchelor and Bowden (1985) (Fig. 9), GEG plots in 'Anorogenic' and 'Post-orogenic' granitoids fields which mainly include A-type granites. Based on these observations, a few conclusions can be made.

- The GEG is highly fractionated. High Ga concentrations have been considered as a diagnostic feature of A-type granites by many investigators (e.g., Collins et al., 1982; Whalen et al., 1987; Eby, 1990; Haapala and Ramo, 1990; Whalen and Currie, 1990). As stated by Whalen et al. (1987), Sawka et al. (1990) and Chappell and White (1992), high fractionation of I- and S-type granites could enrich Ga in the magma. So high Ga concentration is not exclusively a feature of A-type granites.

- The GEG most probably is not S-type, as S-type granites have high concentrations of P_2O_5 which increase with fractionation in this type of granite (Sawka et al., 1990; Chappell and White, 1992). Very low concentrations of P_2O_5 in the GEG and rarity of apatite in hydrothermal assemblages of the Glen Eden prospect indicate a low content of this component in the GEG melt.
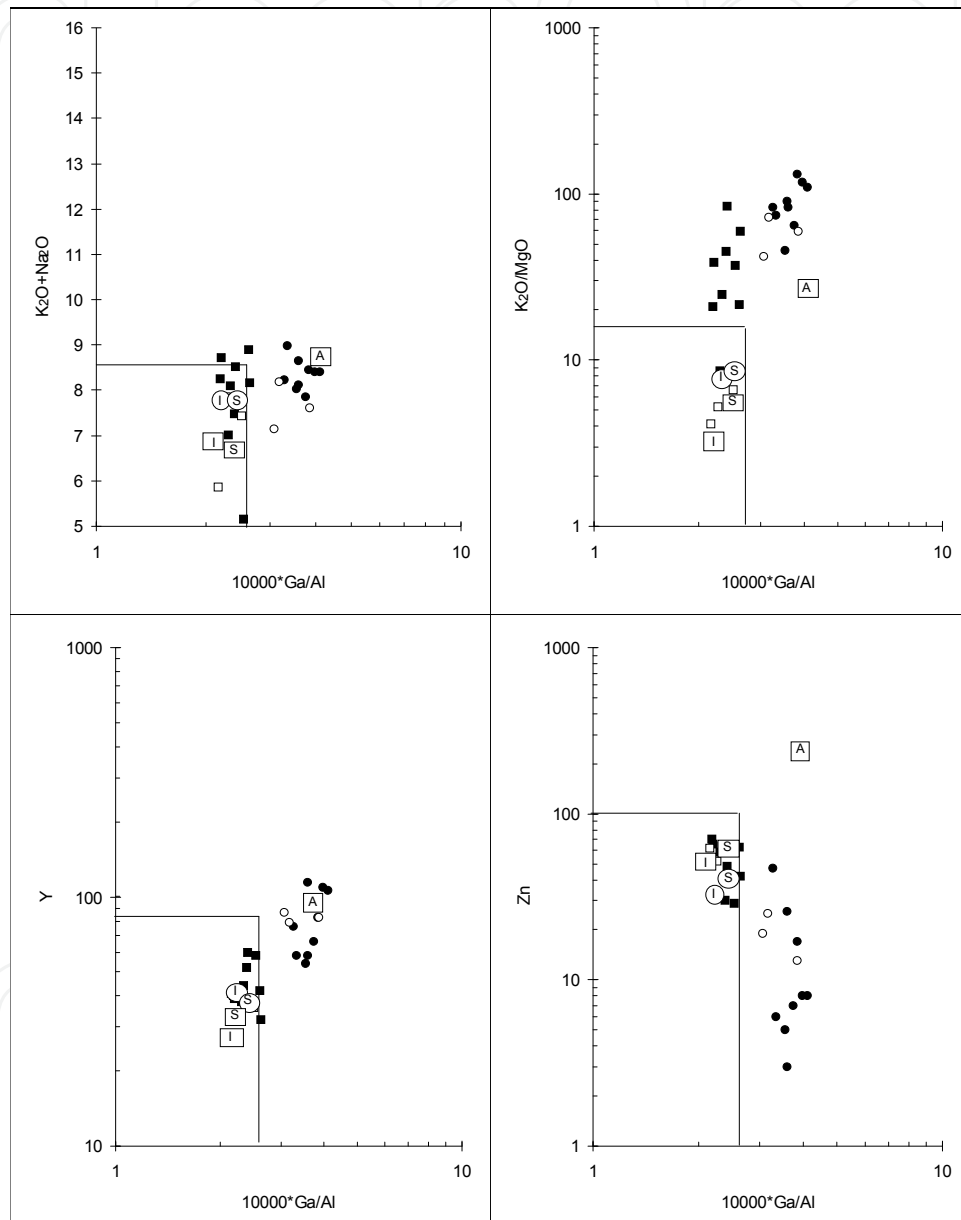- The discrimination diagrams (Figs 8 and 9) cannot unequivocally classify the GEG. There are two main possibilities.

Fig. 7. Data from the GEG and Emmaville Volcanics in discrimination diagrams of Whalen et al. (1987), showing the possible A-type characteristics of this granite. [I] I-type granite average, [S] S-type granite average, (I) felsic I-type granite average, (S) felsic S-type granite average, [A] A-type granite average. . Oxides and trace elements are in percent and ppm, respectively. Closed circle = granite porphyry, open circle = micrographic granite, closed square = rhyolite, open square = dacite and rhyodacite.
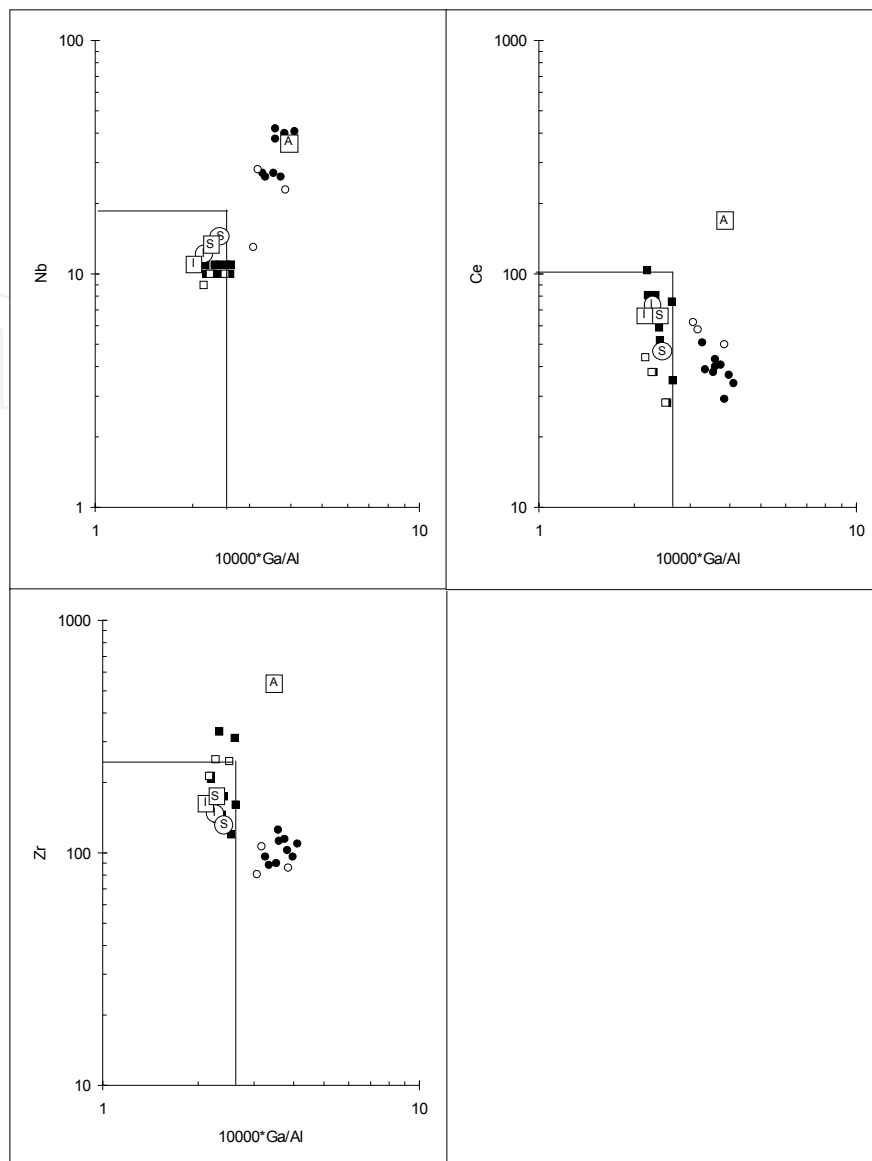
Cont. Fig. 7.

a. The GEG is A-type. In this case, very low concentrations of Zr and Zn (Fig. 10) could be
    due to low concentrations of these elements in the source rocks or a result of
    peraluminousity of the GEG, as non-peralkaline granites contain much lower Zr and Zn
    than peralkaline types. Watson and Harrison (1983) stated that peralkaline melts in
    comparison with peraluminous ones can maintain extremely high zircon solubility by
    complexing Zr^{4+} with free alkalies that are not associated with Al. High mobility of Zn
    during hydrothermal alterations may account for its low concentrations in the GEG.

b. The GEG is fractionated I-type: It has been found that a large degree of fractional
    crystallization of I- and even S-type granite magmas can produce a minor amount of
    evolved magma with high Ga/Al, very low concentrations of Ba and Sr and large
    variation in Rb/Sr and Rb/Ba ratios (Whalen and Currie, 1990). As can be seen in Table
    3, fractionation of I-type granite magmas in the Lachlan Fold Belt increased SiO_2, Rb,
    Pb, Th, U, Nb, Y, Ce, Ga, Sn, DI, Rb/Sr, Rb/Ba and partially Na_2O and K_2O and
    decreased TiO_2, Al_2O_3, Fe_2O_3, FeO, MnO, MgO, CaO, P_2O_5, Ba, Sr, Zr, Sc, V, Ni, Cr, Co,
    Cu, and Zn. Also, with fractionation, the Fe_2O_3/FeO ratio increases (Fig. 11). So it seems

that fractionation of I-type granitic magma could produce the GEG. This is consistent with the field occurrences of the GEG as dykes. These dykes may represent the last stage of fractional crystallization of a major pluton at greater depth.
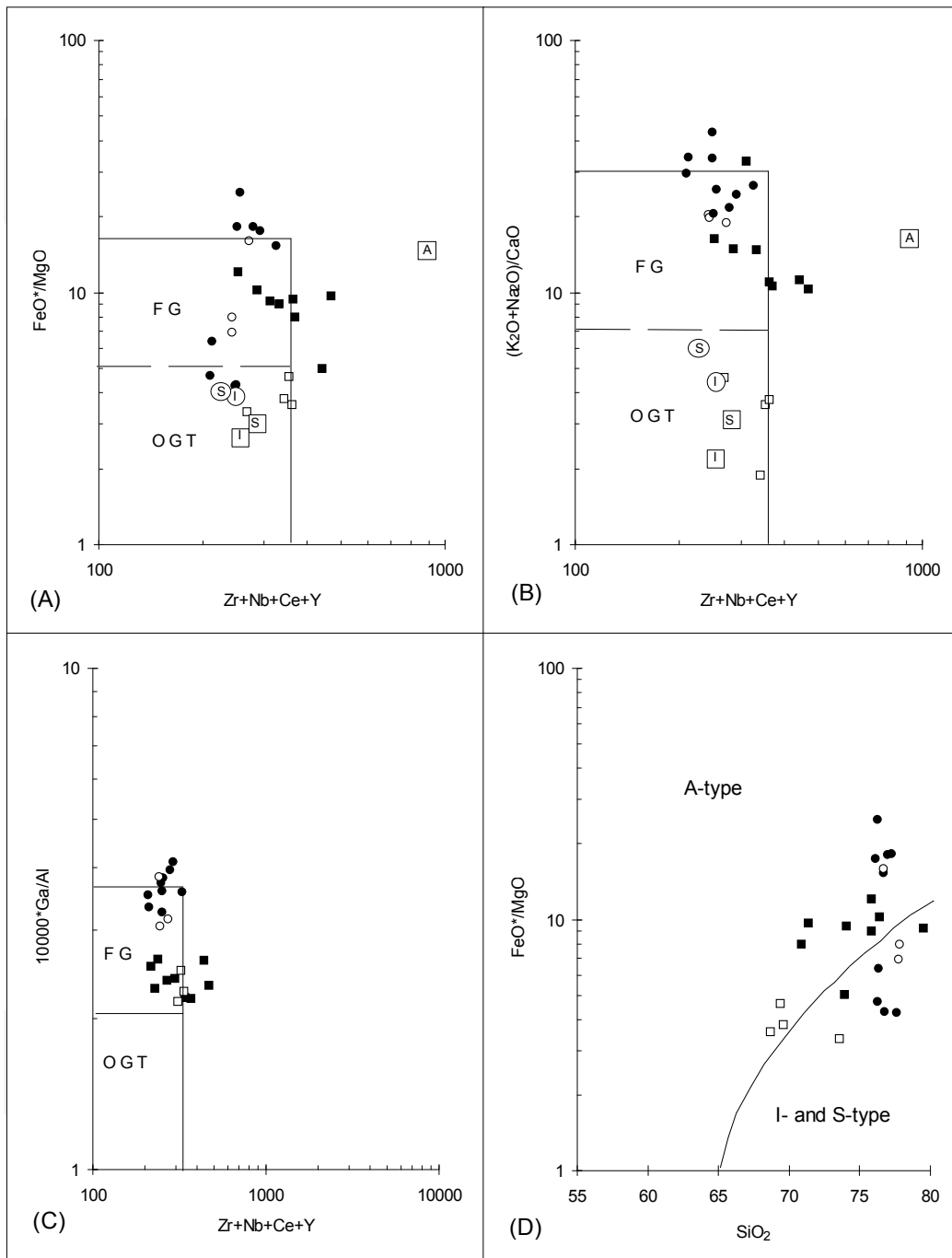
Fig. 8. The GEG and Emmaville Volcanics in discrimination diagrams of Whalen et al. (1987) (A and B) and Eby (1990) (C and D) plot in 'Fractionated Granites' and 'A-type Granites' fields. FeO*= total FeO, F G = Fractionated felsic Granite, O G T = Unfractionated Granite. Oxides and trace elements are in percent and ppm, respectively. Closed circle = granite porphyry, open circle = micrographic granite, closed square = rhyolite, open square = dacite and rhyodacite..
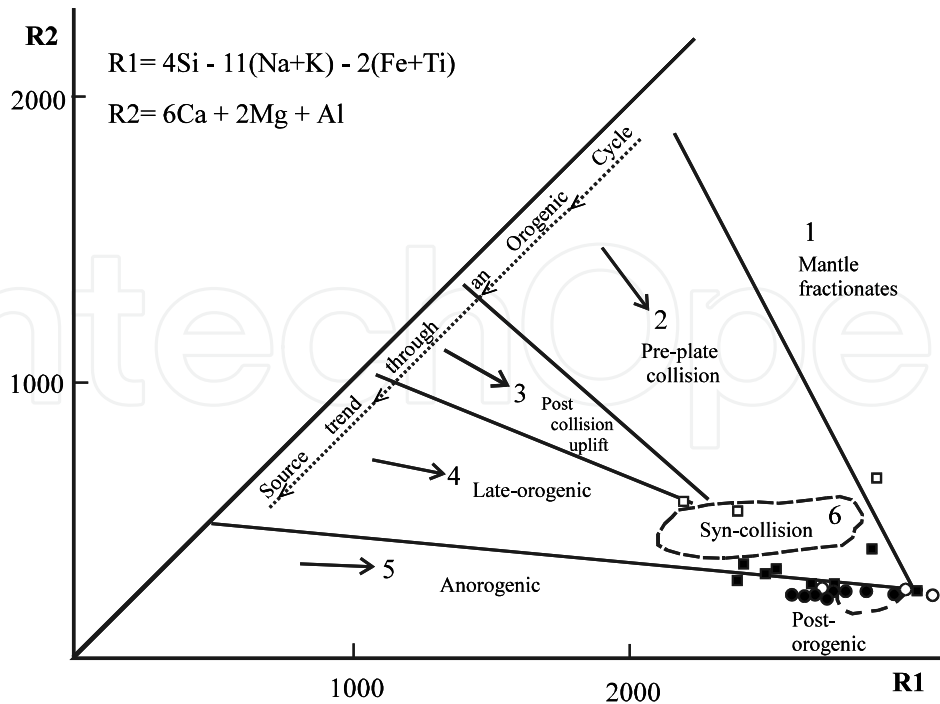
Fig. 9. Data from the GEG and Emmaville Volcanics in the multicationic discrimination diagram for the major granitoids (after Batchelor and Bowden, 1985). Analyzed samples plot mainly in the 'Post Orogenic' and 'Anorogenic' fields. Closed circle = granite porphyry, open circle = micrographic granite, closed square = rhyolite, open square = dacite and rhyodacite.
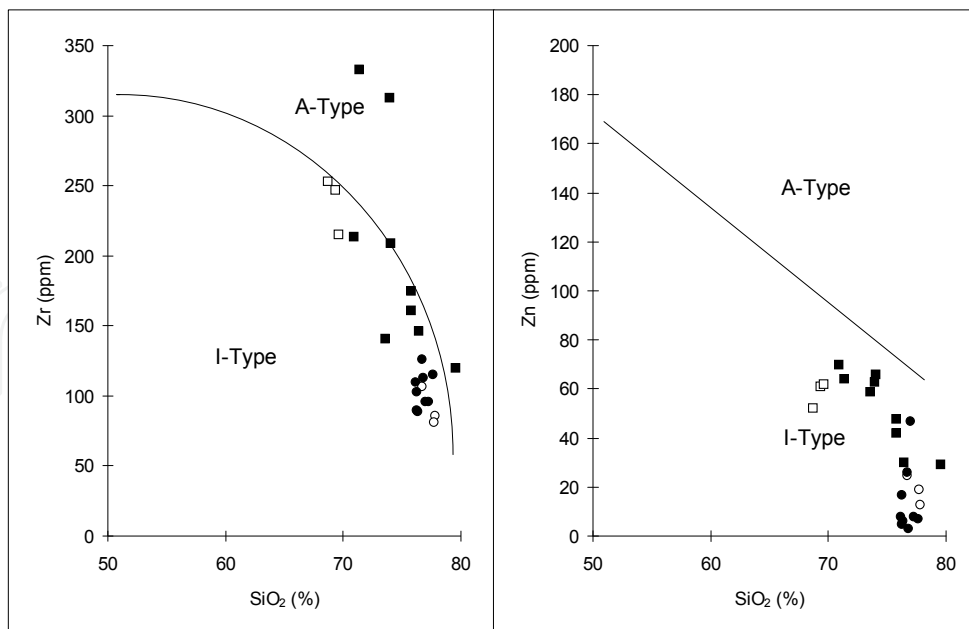
Fig. 10. Data from GEG and Emmaville Volcanics in Zr-SiO$_2$ and Zn-SiO$_2$ diagrams (after Newberry et al., 1990). Low concentrations of Zr and Zn in the GEG cause GEG to plot in the I-type field. Closed circle = granite porphyry, open circle = micrographic granite, closed square = rhyolite, open square = dacite and rhyodacite.
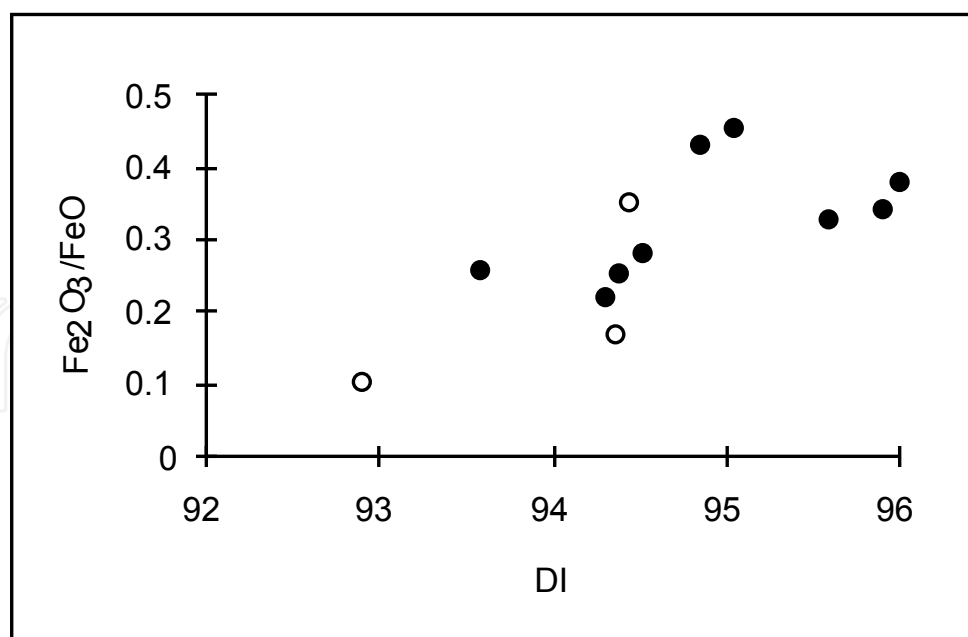
Fig. 11. Plot of DI versus Fe_2O_3/FeO for the GEG, showing increasing Fe_2O_3/FeO with fractionation. Open circle = micrographic granite, closed circle = granite porphyry.

Due to removal of some feldspars and accessory minerals, these dykes show low concentrations of CaO, Sr, Ba, Zr, Zn and high concentrations of U, Th, Nb, Rb, Y, Ga and W. This is consistent with field evidence of other granites associated with Mo-Sn-W ore deposits, wherein fine-grained granites mostly occur as 'carapace' facies formed near the upper contacts of the pluton (e.g., at Krusne hory, Erzgebirge; Stemprok, 1985), or as dyke-like products at the apical part of the larger plutons (Tischendorf, 1977; Blevin and Chappell, 1996a). Either way, fine-grained granites as marginal carapace (Plimer, 1987) or as late-stage phases (Stemprok, 1990; Blevin and Chappell, 1995, 1996a) are one of the common features of plutons associated with Sn, W and Mo ore deposits. Most of these plutons show vertical zoning as enrichment in some elements such as W, Be, Sn, F, Cs, Rb and Li at the top with an impoverishment of Ba, Sr, Ni, Cr and V (Tischendorf, 1977). It is noteworthy that the GEG contains high concentrations of Ni, relative to fractionated I- and A-type granite compositions, which are inconsistent with normal fractionation, as Ni concentration decreases with fractionation. Since Ni is relatively immobile, it is unlikely that this element has been added during slight hydrothermal alteration. It is more likely that the high concentrations of Ni and low concentrations of Ce, La, and Sn in the GEG, relative to other fractionated I-type granites, reflect the compositional features of the source.

Regarding the classification of Ishihara (1977), the GEG has formed under reduced conditions (Fig. 12) and belongs to the ilmenite series, since its Fe_2O_3/FeO ratio is <0.5 (Ishihara, 1981). Generally, I-type granites show higher f_{O_2} than S-types and Chappell and White (1992) consider this feature to be inherited from the source. The GEG shows a wide range of Fe_2O_3/FeO, overlapping with unfractionated and fractionated I- and S-type granites. Fe_2O_3/FeO ratio increases with fractionation in the GEG samples (Table 3, Fig. 11).

In summary, the highly fractionated character of the GEG makes classification difficult. The geochemical features and field observations show that GEG could be A-type or fractionated I-type. As stated by Chappell and White (1992), fractionated I-type granites are similar to fractionated A-types and they can be mistaken.
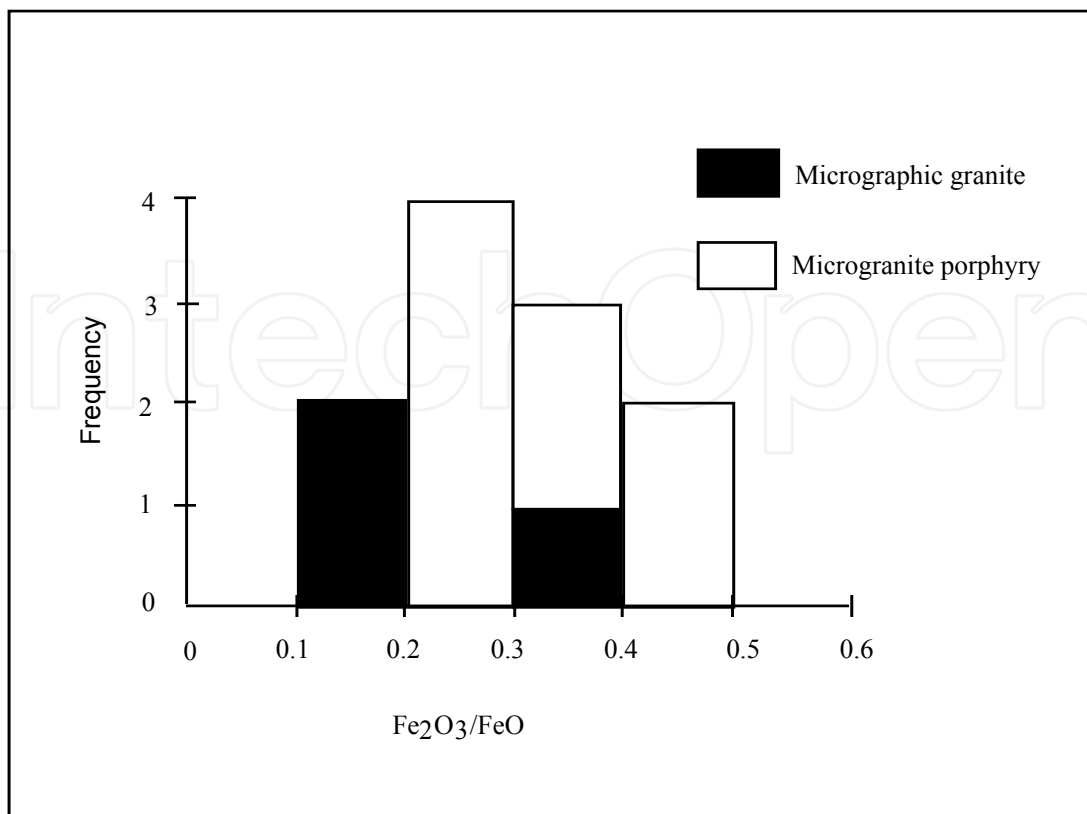
Fig. 12. Histogram of Fe_2O_3/FeO in the GEG, showing the reduced character of the Glen Eden Granite.

6. Tectonic setting

On tectonic discrimination diagrams of Pearce et al. (1984), data from the GEG, but not the associated volcanics, mostly plot in the 'Within Plate' field (Fig. 13). This is typical for A-type granites (Pearce et al., 1984; Whalen et al., 1987), but does not mean that the GEG is necessarily A-type (Whalen and Currie, 1990). Although I- and S-type granites mostly plot in the 'Volcanic Arc' field (Whalen et al., 1987), they may also plot in the 'Within Plate' field (Whalen, 1988). It seems that the high fractionation of I-type granites would increase the concentrations of Nb, Y and Rb and would cause these rocks to plot in the 'Within Plate' field. For example, average fractionated I-type granites of the Lachlan Fold Belt (Table 3) plot in the 'Within Plate' field, as does the GEG.

There seems to be general agreement that A-type granites were emplaced into tensional (or non-compressive) environments either at the end of an orogenic cycle in continental rift zones or in oceanic basins (Eby, 1990). The Glen Eden Granite plots in 'Post-orogenic' and 'Anorogenic' fields on the multicationic diagram of Batchelor and Bowden (1985) (Fig. 9) and it seems that this granite was emplaced into an unstable active margin. This tectonic setting is similar to that proposed for the A-type Topsails Granite, western Newfoundland (Whalen and Currie, 1990).

7. Summary

The various features of the GEG can be summarized as follows.

- The compositional features of the GEG are enrichment in SiO_2, Rb, U, Th, Nb, Y, Ga and W and impoverishment in CaO, P_2O_5, Ba, Sr, Zr and Zn and high values and wide range of Rb/Ba and Rb/Sr.
- The GEG, like other mineralization-associated plutons of the New England Batholith (Kleeman, 1978; Blevin and Chappell, 1996a, b; Vickery et al., 1997), is a high-level leucogranite of near minimum melt composition.
- The presence of crenulate quartz layers, micrographic texture and hydrothermal breccia at Glen Eden suggests saturation of magma from water and the presence of fluid-rich environment.
- The highly fractionated character of the GEG does not allow unequivocal classification but it has strong similarities to fractionated I-type and A-type granites.
- The tectonic setting of the GEG, based on geochemical criteria, is 'Within Plate' and possibly it has been emplaced into an unstable active margin.
- Strong fractionation of the granitic magma increased concentration of incompatible elements, including metals such as Sn, W and Mo, in the final melt and magmatic solution. Increasing the pressure of this fluid eventually caused brecciation of the cap rocks and formed a breccia pipe wherein Mo-W-Sn mineralization occurred.

8. References

Augustithis, S.S. 1973. Atlas of the textural pattern of granites, gneisses and associated rock types. Elsevier, Amsterdam, London, New York, 378pp.

Avila-Salinas, W.A. 1990. Tin-bearing granites from the Cordillera Real, Bolivia: a petrological and geochemical review. Geol. Soc. Am., Special Paper, 145-159.

Bailey, J.C. 1977. Fluorine in granitic rocks and melts: a review. Chem. Geol., 19, 1-42.

Bampton, M.D. 1988. Alteration and mineralisation of the southern part of the Stanthorpe Adamellite, near Tenterfield, New South Wales. Unpublished BSc (Hons) thesis, University of Sydney, 163pp.

Bankwitz, P. 1978. Remarks concerning the development of the Erzgebirge pluton. In M. Stemprok, L. Burnol and G. Tischendorf (eds), Metallization associated with acid magmatism, 3, 156-167.

Batchelor, R.A. and Bowden, P. 1985. Petrogenetic interpretation of granitoid rock series using multicationic parameters. Chem. Geol., 48, 43-55.

Blevin, P.L. and Chappell, B.W. 1995. Chemistry, origin, and evolution of mineralized granites in the Lachlan Fold Belt, Australia: the metallogeny of I- and S-type granites. Econ. Geol., 90, 1604-1619.

Blevin, P.L. and Chappell, B.W. 1996a. Internal evolution and metallogeny of Permo-Triassic high-K granites in the Tenterfield-Stanthorpe region, southern New England Orogen, Australia. In Mesozoic geology of the eastern Australia plate conference, Geol. Soc. Aust., Abs., 43, 94-100.

Blevin, P.L. and Chappell, B.W. 1996b. Permo-Triassic granite metallogeny of the New England Orogen. In Mesozoic geology of the eastern Australia plate conference, Geol. Soc. Aust., Abs., 43, 101-103.

Brodie, R.S. 1983. Geology and mineralization of the Mole River-Silent Grove area, near Tenterfield, northern New South Wales. Unpublished BSc (Hons) thesis, University of New England, 149pp.

Burnham, C.W. 1967. Hydrothermal fluids in the magmatic stage. In H.L. Barnes (ed), Geochemistry of hydrothermal ore deposits, New York, John Wiley, 34-76.

Burnham, C.W. 1979. Magmas and hydrothermal fluids. In H.L. Barnes (ed), Geochemistry of hydrothermal ore deposits, 2nd edition, New York, John Wiley, 71-136.

Carmichael, I.S.E., Turner, F.J. and Verhoogen, J. 1974. Igneous Petrology. New York. McGraw-Hill Book Co., 739pp.

Carten, R.B., Walker, B.M., Geraghty, E.P. and Gunow, A.J. 1988. Comparison of field-based studies of the Henderson porphyry molybdenum deposit, Colorado, with experimental and theoretical models of porphyry systems. In R.P. Taylor and D.F. Strong (eds), Recent advances in the geology of granite-related mineral deposits, Can. Ins. Min. Metall., 39, 1-12.

Chappell, B.W. and White, A.J.R. 1992. I- and S-type granites in the Lachlan Fold Belt. Trans. Roy. Soc. Edin.: Earth Sci., 83, 1-26.

Collins, W.J., Beams, S.D., White, A.J.R. and Chappell, B.W. 1982. Nature and origin of A-type granites with particular reference to southeastern Australia. Contrib. Mineral. Petrol., 80, 189-200.

Collins, W.J., Offler, R., Farrell, T.R. and Landenberger, B. 1993. A revised Late Palaeozoic-Early Mesozoic tectonic history for the southern New England Fold Belt. In P.G. Flood and J.C. Aitchison (eds), New England Orogen, eastern Australia, University of New England, 69-84.

Dingwell, D.B. 1985. The structure and properties of fluorine-rich silicate melts: implications for granite petrogenesis. In R.P. Taylor and D.F. Strong (eds), Granite-related mineral deposits geology, petrogenesis and tectonic setting, CIM Conference on Granite-related Mineral Deposits, 72-81.

Dingwell, D.B. 1988. The structure and properties of fluorine-rich magmas: a review of experimental studies. In R.P. Taylor and D.F. Strong (eds), Recent advances in the geology of granite-related mineral deposits. Can. Inst. Min. Metall., Special Volume 39, 1-12.

Dingwell, D.B., Scarfe, C.M. and Cronin, D.J. 1985. The effect of fluorine on viscosities in the system Na_2O-Al_2O_3-SiO_2 - implications for phonolites, trachytes and rhyolites. Am. Mineral., 70, 80-87.

Eby, G.N. 1990. The A-type granitoids: a review of their occurrence and chemical characteristics and speculations on their petrogenesis. In A.R. Woolley and M. Ross (eds), Alkaline igneous rocks and carbonatites. Lithos, 26, 115-134.

Fenn, P.M. 1979. On the origin of graphic intergrowth [abs.]. Geol. Soc. Am., Abstr. Programs, 11, 424.

Flood, P.G. and Aitchison, J.C. 1993a. Understanding New England geology: the comparative approach. In P.G. Flood and J.C. Aitchison (eds), New England Orogen, eastern Australia, University of New England, 1-10.

Flood, P.G. and Aitchison, J.C. 1993b. Recent advances in understanding the geological development of the New England Province of the New England Orogen. In P.G. Flood and J.C. Aitchison (eds), New England Orogen, eastern Australia, University of New England, 61-67.

Glyuk, D.S. and Anfiligov, V.N. 1973. Phase equilibria in the system granite-H_2O-HF at a pressure of 1000 kg/cm^2. Geochem. Internat., 10, 313-317.

Haapala, I. and Ramo, O.T. 1990. Petrogenesis of the Proterozoic rapakivi granite of Finland. In H.J. Stein and J.L. Hannah (eds), Ore-bearing granite systems ; petrogenesis and mineralizing processes. Geol. Soc. Am., Special Paper, 246, 275-286.

Hannah, J.L. and Stein, H.J. 1990. Magmatic and hydrothermal processes in ore bearing systems. In H.J. Stein and J.L. Hannah (eds), Ore-bearing granite systems; petrogenesis and mineralizing processes. Geol. Soc. Am., Special Paper, 246, 1-10.

Hensel, H.D. 1982. The mineralogy, petrology and geochronology of granitoids and associated intrusives from the southern portion of the New England Batholith. Unpublished Ph.D. thesis, University of New England, 273pp.

Holtz, F., Pichavant, M., Barbey, P. and Johannes, W. 1992. Effects of H_2O on liquidus phase relations in the haplogranite system at 2 and 5 kbar. Am. Mineral., 77, 1223-1241.

Ishihara, S. 1977. The magnetite-series and ilmenite-series granitic rocks. Min. Geol., 27, 293-305.

Ishihara, S. 1981. The granitoid series and mineralization. Econ. Geol., 75th Anniversary Volume, 458-484.

Keith, J.D. and Shanks, W.C. 1988. Chemical evolution and volatile fugacities of the Pine Grove porphyry molybdenum and ash-flow tuff system, southwestern Utah. In R.P. Taylor and D.F. Strong (eds), Recent advances in the geology of granite-related mineral deposits. Can. Inst. Min. Metall., Special Volume, 39, 402-423.

Keppler, H. 1993. Influence of fluorine on the enrichment of high field strength trace elements in granitic rocks. Contrib. Mineral. Petrol., 114, 479-488.

Kirkham, R.V. and Sinclair, W.D. 1988. Comb quartz layers in felsic intrusions and their relationship to porphyry deposits. In R.P. Taylor and D.F. Strong (eds), Recent advances in the geology of granite-related mineral deposits. Can. Inst. Min. Metall., Special Volume, 39, 50-71.

Kleeman, J.D. 1978. Tin mineralizing granites in New England [abs]. Australian Geology Convention, 3rd, Townsville, August 1978, Abstracts and Programs, 37.

Kleeman, J.D. 1982. The anatomy of a tin-mineralizing A-type granite. In P.G. Flood and B. Runnegar (eds), New England Geology., University of New England and AHV Club, 327-334.

Kontak, D.J. 1994. Geological and geochemical studies of alteration processes in a fluorine-rich environment: the east Kemptville Sn-(Zn-Cu-Ag) deposit, Yarmouth Country, Nova Scotia, Canada. In D.R. Lentz (ed), Alteration and alteration processes associated with ore-forming systems, Geological Association of Canada, Short Course Notes, 11, 261-314.

Kovalenko, V.I., Kuz'min, M.I., Antipin, V.S. and Petrov, L.L. 1971. Topaz bearing keratophyre (ongonite), a new variety of subvolcanic igneous vein rock. Doklady Academy Science, U. S. S. R., Earth Science Section, 199, 132-135.

Le Maitre, R.W. 1976. The chemical variability of some common igneous rocks, Jour. Petrology, 17, 589-637.

Le Messurier, L.A. 1983. The genetic relationships between two alkali granites and associated enclosing I-type plutons within the New England region. Unpublished BSc (Hons) thesis, University of New England, 131pp.

London, D. 1987. Internal differentiation of rare-element pegmatites: effects of boron, phosphorus, and fluorine. Geochim. et Cosmochim. Acta, 51, 403-420.

Luth, W.C. 1976. Granitic rocks. In D.K. Bailey and R. Macdonald (eds), The evolution of the crystalline rocks, Academic Press, London, 335-417.

Manning, D.A.C. 1981. The effect of fluorine in liquidus phase relationships in the system Qz-Ab-Or with excess water at 1 kb. Contrib. Mineral. Petrol., 76, 206-215.

Manning, D.A.C. and Pichavant, M. 1988. Volatiles and their bearing on the behavior of metals in granitic systems. In R.P. Taylor and D.F. Strong (eds), Recent Advances in the Geology of Granite-Related Mineral Deposits, Can. Ins. Min. Metall., Special Volume, 39, 13-24.

Moore, J.G. and Lockwood, J.P. 1973. Origin of comb layering and orbicular structure, Sierra Nevada Batholith, California. Geol. Soc. Am. Bull., 48, 1-20.

Munoz, J.L. and Ludington, S.D. 1974. Fluorine-hydroxyl exchange in biotite. Am. Jour. Sci., 274, 396-413.

Murray, C.G. 1988. Tectonic evolution and metallogenesis of the New England Orogen. In J.D. Kleeman (ed), New England Orogen - tectonics and metallogenesis. University of New England, 204-210.

Nabelek, P.I. and Russ-Nabelek, C. 1990. The role of fluorine in the petrogenesis of magmatic segregations in the St. Francois volcano-plutonic terrane, southeastern Missouri. In H.J. Stein and J.L. Hannah (eds), Ore-bearing granite systems; petrogenesis and mineralizing processes. Geol. Soc. Am., Special Paper, 246, 71-87.

Newberry, R.J., Burns, L.E., Swanson, S.E. and Smith, T.E. 1990. Comparative petrologic evolution of the Sn and W granites of the Fairbanks-Circle area, interior Alaska. In H.J. Stein and J.L. Hannah (eds), Ore-bearing granite systems; petrogenesis and mineralizing processes. Geol. Soc. Am., Special Paper, 246, 121-142.

Nockolds, S.R. 1954. Average chemical compositions of some igneous rocks. Geol. Soc. Am. Bull., 65, 1007-1032.

Pearce, J.A., Harris, N.B.W. and Tindle, A.J. 1984. Trace elements discrimination diagrams for the tectonic interpretation of granitic rocks. Jour. Petrology, 25, 956-983.

Pichavant, M. and Manning, D. A. C. 1984. Petrogenesis of tourmaline granites and topaz granites; the contribution of experimental data. Physics of the Earth and Planetary Interiors, 35, 31-50.

Plimer, I.R. and Kleeman, J.D. 1985. Mineralization associated with the Mole Granite, Australia. In: High heat production (HHP) granites, hydrothermal circulation and ore genesis. St. Austell, England, Inst. Mining Metallurgy, 563-570.

Plimer, I.R. 1973. The pipe deposits of tungsten-molybdenum-bismuth in eastern Australia. Unpublished PhD. thesis, Macquarie University, 288pp.

Plimer, I.R. 1987. Fundamental parameters for the formation of granite-related tin deposits. Geologische Rundschau, 76, 23-40.

Povilaitis, M.M. 1978. Effect of the conditions of magmatic emplacement on high-temperature postmagmatic ore mineralization. In M. Stemprok, L. Burnol and F. G. Tischendorf, Metallization associated with acid magmatism, 3, 375-384.

Richardson, J.M., Bell, K., Watkinson, D.H. and Blenkinsop, J. 1990. Genesis and fluid evolution of the East Kemptville greisen-hosted tin mine, southwestern Nova Scotia, Canada. In H.J. Stein and J.L. Hannah (eds), Ore-bearing granite systems; petrogenesis and mineralising processes. Geol. Soc. Am., Special Paper, 246, 181-203.

Sawka, W.N., Heizler, M.T., Kistler, R.W. and Chappell, B.W. 1990. Geochemistry of highly fractionated I- and S-type granites from the tin-tungsten provinces of western Tasmania. In H.J. Stein and J.L. Hannah (eds), Ore-bearing granite systems; petrogenesis and mineralizing processes. Geol. Soc. Am., Special Paper, 246, 161-179.

Schroecke, H. 1973. Grundlagen der magmatogenen lagerstättenbildung. Enke Verlag. Stuttgart, 287pp.

Shaver, S.A. 1984a. Origin of crenulate quartz layers - evidence from the Hall (Nevada Moly) molybdenum deposit, Nevada [abs]. Geol. Soc. Am., Abstr. Programs, 16, 254-255.

Shaver, S.A. 1984b. The Hall (Nevada Moly) molybdenum deposit, Nye Country, Nevada: geology, alteration, mineralization and geochemical dispersion. Unpublished Ph.D. thesis, Stanford Univ., 261pp.

Shaw, S.E. and Flood, R.H. 1981. The New England Batholith, eastern Australia: geochemical variations in space and time. Jour. Geoph. Res., 86, 10530-10544.

Sheppard, S.M.F. 1977. Identification of the origin of ore-forming solutions by the use of stable isotopes. In: Volcanic processes in ore genesis, Geol. Soc. London, Special. Publication, 7, 25-41.

Somarin, A.K. 1999. Mineralogy, geochemistry and genesis of the Glen Eden Mo-W-Sn deposit, New England Batholith, Australia. Unpublished PhD thesis, University of New England, Armidale, Australia, 340pp.

Somarin, A.K., and Ashley, P., 2004. Hydrothermal alteration and mineralization of the Glen Eden Mo-W-Sn deposit: a leucogranite-related hydrothermal system, Southern New England Orogen, NSW, Australia. Mineralium Deposita, 39, 282-300.

Stegman, C.L. 1983. The Mole Granite and its Sn-W-Mo-base metal mineralization - a study of its southern-central margin. Unpublished BSc (Hons) thesis, University of New England, 177pp.

Stemprok, M. 1985. Vertical extent of greisen mineralization in the Krusne hory/Erzgebirge granite pluton of central Europe. In: High heat production (HHP) granites, hydrothermal circulation and ore genesis. St. Austell, England, Inst. Mining Metallurgy, 41-54.

Stemprok, M. 1990. Intrusion sequences within ore-bearing granitoid plutons. Geological Jour., 25, 413-417.

Stewart, J.P. 1983. Petrology and geochemistry of the intrusives spatially associated with the Logtung W-Mo prospect, south-central Yukon Territory. Unpublished M.Sc. thesis, University of Toronto, 243pp.

Strong, D.F. 1988. A review and model for granite-related mineral deposits. In R.P. Taylor and D.F. Strong (eds), Recent advances in the geology of granite-related mineral deposits. Can. Inst. Min. Metall., Special Volume, 39, 424-445.

Stroud, W.J. 1995. Inverell 1: 250000 metallogenic map.

Taylor, R.P. 1992. Petrological and geochemical characteristics of the Pleasant Ridge zinnwaldite-topaz granite, southern New Brunswick, and comparison with other topaz-bearing felsic rocks. Can. Mineral., 30, 895-921.

Tischendorf, G. 1977. Geochemical and petrographic characteristics of silicic magmatic rocks associated with rare-element mineralization. In M. Stemprok, L. Burnol and G. Tischendorf (eds), Metallization associated with acid magmatism, 2, 41-96.

Tuttle, O.F. and Bowen, N.L. 1958. Origin of granite in the light of experimental studies in the system $NaAlSi_3O_8$-$KAlSi_3O_8$-SiO_2-H_2O. Geol. Soc. Am. Mem., 74.,153pp.

Velde, B. and Kushiro, I. 1978. Structure of sodium aluminosilicate melts quenched at high pressure; infrared and aluminum K radiation data. Earth Planet. Sci. Lett., 40, 137-140.

Vickery, N.M., Ashley, P.M. and Fanning, C.M. 1997. Dumboy-Gragin Granite, northeastern New South Wales: age and compositional affinities. In P.M. Ashley and P.G. Flood (eds), Tectonics and Metallogenesis of the New England Orogen, Geological Society of Australia Special Publication, 19, 266-271.

Walsh, J. 1991. Two distinctive granitoids from the Copeton region: a mineralogical, geochemical and mineralization study. Unpublished BSc (Hons) thesis, University of New England, 200pp.

Watson, E.B. and Harrison, T.M. 1983. Temperature and compositional effects in a variety of crustal magma type. Earth Planet. Sci. Lett., 64, 295-304.

Webster, J.D. and Holloway, J.R. 1990. Partitioning of F and Cl between magmatic hydrothermal fluid and highly evolved granitic magmas. In H.J. Stein and J.L. Hannah (eds), Ore-bearing granite systems; petrogenesis and mineralizing processes. Geol. Soc. Am., Special Paper, 246, 21-34.

Whalen, J.B. and Currie, K.L. 1990. The Topsails igneous suite, western Newfoundland, fractionation and magma mixing in an "orogenic" A-type granite suite. In H.J. Stein and J.L. Hannah (eds), Ore-bearing granite systems; petrogenesis and mineralizing processes. Geol. Soc. Am., Special Paper, 246, 287-299.

Whalen, J.B., Currie, K.L. and Chappell, B.W. 1987. A-type granites; geochemical characteristics, discrimination, and petrogenesis. Contrib. Mineral. Petrol., 95, 407-419.

Whalen, J.B. 1988. Granitic rocks of New Brunswick and Gaspe, Quebec: a transect across the southern Canadian Appalachians. Geol. Assoc. Can. Prog. Abst., 13, A133.

White, W.H., Bookstrom, A.A., Kamilli, R.J., Ganster, M.W., Smith, R.P., Ranta, D.E. and Steininger, R.C. 1981. Character and origin of Climax-type molybdenum deposits. Econ. Geol., 75th Anniversary Volume, 270-316.

Winkler, H.G.F. 1974. Petrogenesis of Metamorphic Rocks. Berlin, Springer Verlag.

Wyllie, P.J. 1979. Magmas and volatile components. Am. Mineral., 64, 469-500.

Zen, E. 1986. Aluminum enrichment in silicate melts by fractional crystallization, some mineralogic and petrographic constraints. Jour. Petrology, 27, 1095-1117.

Earth and Environmental Sciences

Edited by Dr. Imran Ahmad Dar

We are increasingly faced with environmental problems and required to make important decisions. In many cases an understanding of one or more geologic processes is essential to finding the appropriate solution. Earth and Environmental Sciences are by their very nature a dynamic field in which new issues continue to arise and old ones often evolve. The principal aim of this book is to present the reader with a broad overview of Earth and Environmental Sciences. Hopefully, this recent research will provide the reader with a useful foundation for discussing and evaluating specific environmental issues, as well as for developing ideas for problem solving. The book has been divided into nine sections; Geology, Geochemistry, Seismology, Hydrology, Hydrogeology, Mineralogy, Soil, Remote Sensing and Environmental Sciences.

How to reference

In order to correctly reference this scholarly work, feel free to copy and paste the following:

A. K. Somarin (2011). Petrography, Geochemistry and Petrogenesis of Late-Stage Granites: An Example from the Glen Eden Area, New South Wales, Australia, Earth and Environmental Sciences, Dr. Imran Ahmad Dar (Ed.), ISBN: 978-953-307-468-9, InTech, Available from: http://www.intechopen.com/books/earth-and-environmental-sciences/petrography-geochemistry-and-petrogenesis-of-late-stage-granites-an-example-from-the-glen-eden-area-

INTECH
open science | open minds